

FlowMoE: A Scalable Pipeline Scheduling Framework for Distributed Mixture-of-Experts Training

**Yunqi Gao¹, Bing Hu^{1*}, Mahdi Boloursaz Mashhadi², A-Long Jin³, Yanfeng Zhang⁴,
Pei Xiao², Rahim Tafazolli², Mérouane Debbah⁵**

¹School of Information Science and Electronic Engineering, Zhejiang University

²5GIC & 6GIC, Institute for Communication Systems (ICS), University of Surrey

³School of Advanced Technology, Xi'an Jiaotong-Liverpool University

⁴School of Computer Science and Engineering, Northeastern University

⁵KU 6G Research Center, Department of Computer and Information Engineering, Khalifa University
{gaoyunqi1999, binghu}@zju.edu.cn,

{m.boloursazmashhadi, p.xiao, r.tafazolli}@surrey.ac.uk,
along.jin@xjtu.edu.cn, zhangyf@mail.neu.edu.cn, merouane.debbah@ku.ac.ae

Abstract

The parameter size of modern large language models (LLMs) can be scaled up via the sparsely-activated Mixture-of-Experts (MoE) technique to avoid excessive increase of the computational costs. To further improve training efficiency, pipelining computation and communication has become a promising solution for distributed MoE training. However, existing work primarily focuses on scheduling tasks within the MoE layer, such as expert computing and all-to-all (A2A) communication, while neglecting other key operations including multi-head attention (MHA) computing, gating, and all-reduce communication. In this paper, we propose FlowMoE, a scalable framework for scheduling multi-type task pipelines. First, FlowMoE constructs a unified pipeline to consistently scheduling MHA computing, gating, expert computing, and A2A communication. Second, FlowMoE introduces a tensor chunk-based priority scheduling mechanism to overlap the all-reduce communication with all computing tasks. We implement FlowMoE as an adaptive and generic framework atop PyTorch. Extensive experiments with 675 typical MoE layers and four real-world MoE models across two GPU clusters demonstrate that our proposed FlowMoE framework outperforms state-of-the-art MoE training frameworks, reducing training time by 13%-57%, energy consumption by 10%-39%, and memory usage by 7%-32%. FlowMoE's code is available at <https://github.com/ZJU-CNLAB/FlowMoE>.

1 Introduction

Large language models (LLMs) have demonstrated remarkable performance on natural language processing (NLP) tasks as model sizes increase (e.g., GPT-3 [1] with 175 billion parameters, LLaMA3.1 [2] with 405 billion parameters, and DeepSeek-R1 [3] with 671 billion parameters). However, parameter scaling causes a linear increase in the computational cost. Currently, sparsely-activated LLMs with Mixture-of-Experts layers (MoE models) have become extremely popular [4], where the MoE layer replaces the standard feed-forward layer in traditional transformer blocks. In MoE, a gating function selects a small subset of dense layers, known as experts, to be activated for the input sample tokens. This dynamic selection enables only a few experts to participate in computation during each iteration [5, 6]. Therefore, MoE techniques can scale the model size with limited increase in computation [5, 7, 8], e.g., Google's Switch Transformer expands parameters from a few billion to 1.5 trillion through 15 MoE layers with 2048 experts each [9]. However, training MoE models on large-scale GPU clusters still suffers from serious scalability bottlenecks [10, 11, 12].

*Corresponding author

Table 1: Time for different tasks of each iteration in training four MoE models on a 16-GPU (NVIDIA RTX3090) cluster (with 100Gbps bandwidth) running vanilla expert parallelism [19]. ‘MHA + Gating Time’ indicates the computing time of the MHA layer and the gating function. ‘All-Reduce Time’ indicates the time of all-reduce communication. ‘Ratio’ indicates the ratio of the sum of ‘MHA + Gating Time’ and ‘All-Reduce Time’ over the total time per iteration.

Model	MHA + Gating Time	All-Reduce Time	Iteration Time	Ratio
GPT2-Tiny-MoE	23.5ms	32.6ms	169.5ms	33.1%
BERT-Large-MoE	61.9ms	98.3ms	537.8ms	29.8%
LLaMA2-MoE	308.4ms	368.8ms	1987.7ms	34.2%
DeepSeek-V2-S	870.2ms	1247.8ms	5843.3ms	36.1%

Recently, expert parallelism has been proposed to train MoE models in a distributed fashion by placing different experts on multiple workers since a single worker (e.g., GPU) cannot hold a complete MoE model [5]. In each iteration, input tokens need to be transferred to particular workers, which depends on an all-to-all (A2A) communication operation (*dispatch*), and the outputs from expert computing on different workers need to be collected via another A2A operation (*combine*) [13]. In addition, the parameters of the remaining parts of the model including the multi-head attention (MHA) layer and the gating function are replicated across all workers to perform data parallelism mode [14, 15, 16, 17, 18]. In particular, the parameters of the MHA layer and the gating function need to be synchronized among all workers using the all-reduce communication after backward propagation.

Since the computing and communication tasks do not occupy the same hardware resources, pipelining of computing and communication becomes one of the most efficient methods for accelerating expert parallelism. Existing works (e.g., ScheMoE [10], Tutel [12], FasterMoE [11], Lina [20], PipeMoE [21], Comet [22]) pipeline expert computing tasks and A2A communication tasks to hide the communication and reduce the training time of the MoE model by splitting the input data of the MoE layer into micro-batches. However, they focus only on overlapping tasks in the MoE layer and neglect MHA layer computing, gating, and all-reduce communication. We conducted experiments on a 16-GPU cluster and the results are shown in Table 1 (see Table 2 for model configurations). It can be observed that the MHA layer computing, gating, and all-reduce communication constitute 30%-40% of the iteration time. Therefore, designing a pipeline scheduling method that considers all major tasks of the transformer block with MoE layer can maximize the overlap between computing and communication, thus improving the scaling efficiency of distributed MoE training.

In this paper, we propose FlowMoE, a scalable pipeline scheduling framework for multi-type tasks in distributed MoE training. We make the following main technical contributions: (1) We construct a unified pipeline that consistently schedules MHA computing, gating, expert computing, and A2A communication. (2) We design a priority-based scheduling mechanism for communication tasks using all-reduce tensor chunks to further overlap the all-reduce communication with computing tasks, and we leverage Bayesian optimization (BO) to automatically tune the partition size of all-reduce chunks. (3) We implement the FlowMoE framework on PyTorch [23] and open-source the code. Extensive experiments on two GPU clusters using manually customized MoE layers and real-world transformer-based MoE models show that FlowMoE achieves better training performance than state-of-the-art MoE frameworks (including ScheMoE [10], FFSMoE [24], Tutel [12] and FasterMoE [11]) and vanilla expert parallelism [19]. Specifically, FlowMoE outperforms ScheMoE by 26% average time efficiency in training 675 MoE layers with different configurations. In comparison with state-of-the-art frameworks in training real-world popular MoE models, FlowMoE achieves $1.13 \times$ - $1.82 \times$ speedup, and reduces energy consumption by 10%-41% and memory usage by 7%-32% during each training iteration. The main differences between FlowMoE and the key literature is shown in Appendix A.

2 Background and Challenges

2.1 Transformer Block with MoE Layer

Fig. 1a illustrates a typical transformer structure with MoE layers, where the transformer block usually consists of an MHA layer and an MoE layer. For the input tensor $I \in \mathbb{R}^{B \times N \times M}$, the MHA layer utilizes the Query, Key, and Value matrices $W^Q, W^K, W^V \in \mathbb{R}^{M \times M}$ to calculate the attention data of each token and obtains the output tensor $I' \in \mathbb{R}^{B \times N \times M}$ through a linear transformation

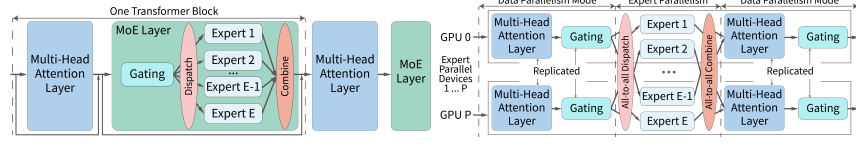


Figure 1: An example of a transformer block with MoE layer and expert parallelism.

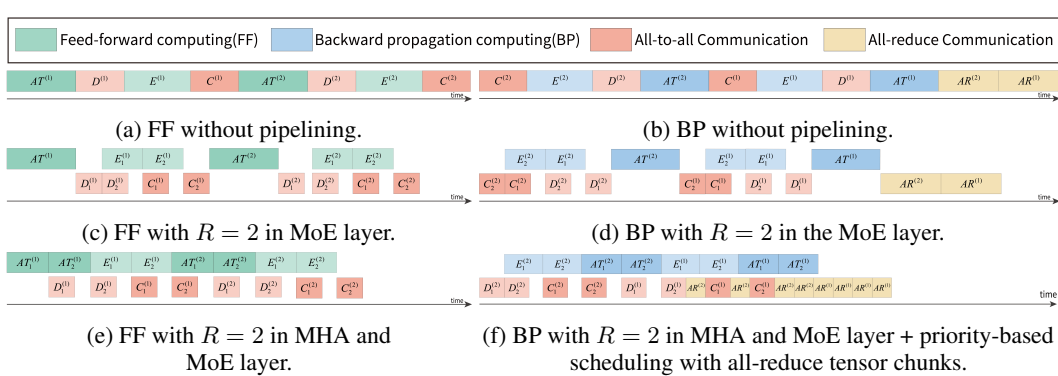


Figure 2: An example of the execution timelines of the computing and communication tasks for a model consisting of two transformer blocks with MoE layer.

matrix $W^O \in \mathbb{R}^{M \times M}$, where B denotes the number of samples per GPU (or mini-batch size) in one iteration, N denotes the number of tokens per sample, and M denotes the embedding size of a token. The MoE layer includes a *gating function* and multiple *experts*. The gating function G is a small learnable neural network followed by a softmax layer and is used to select the activated experts for the input tokens. Typically, only top- k experts are chosen to process a token [9]. The output tensor $G(I') \in \mathbb{R}^{E \times C \times M}$ of the gating function will be dispatched to the corresponding expert (each expert receives a tensor of shape $C \times M$), where E denotes the total number of experts per MoE layer and C denotes the maximum number of tokens assigned to one expert. C can be calculated by $f \times k \times B \times N/E$, where f is the capacity factor that determines the maximum number of tokens assigned to each expert and is used to adjust C [5]. An expert is usually a small neural network with two structurally symmetric feed-forward layers (the first and the second layers are of sizes $M \times H$ and $H \times M$, respectively), where H denotes the hidden size of the feed-forward layer, and each expert is considered to have its own domain of expertise. After expert computing, the outputs from all the experts are combined into a tensor with a shape of $B \times N \times M$ as the input to the next transformer block.

2.2 Expert Parallelism

We define P as the number of workers (or GPUs) in the cluster, L as the number of transformer blocks in a MoE model. Fig. 1b shows an example of training an MoE model on P workers by expert parallelism, where each worker has different expert parameters. Then, $AT_r^{(l)}$, $E_r^{(l)}$, $D_r^{(l)}$, and $C_r^{(l)}$ respectively denote the r th subtask of MHA layer (including gating function), expert computing, dispatch A2A communication, and combining A2A communication of the l th transformer block. $AR^{(l)}$ denotes all-reduce communication task of the l th transformer block. Figs. 2a and 2b show the timelines of multiple computing and communication tasks in the feed-forward computing and backward propagation for one transformer block in vanilla expert parallelism [19]. It is worth noting that the timeline for backward propagation is opposite to that of feed-forward computing, but the parameters of the MHA layer and the gating function need to be synchronized through additional all-reduce communication operation.

2.3 Performance Bottlenecks in Distributed MoE Training

Most of existing pipeline scheduling works (e.g., ScheMoE [10], Tutel [12], PipeMoE [21]) partitions the input token tensor of the MoE layer in the data dimension according to the pipelining degree R , where Figs. 2c and 2d illustrate a pipelining example with $R=2$ in the MoE layer of a transformer block. In addition, FasterMoE [11] splits the input tensor of the MoE layer based on the number of workers, enabling point-to-point communication between workers. Although

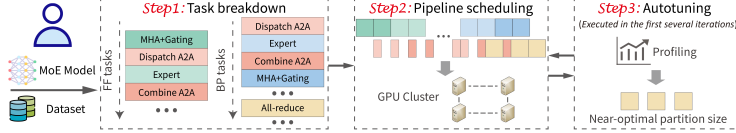


Figure 3: Workflow of FlowMoE.

these works effectively reduce the training time by pipelining the expert computing task and the A2A communication task, they neglect the MHA layer computing task, gating task and all-reduce communication task. Moreover, some MoE frameworks (e.g., FSMoE [24] and Lina [20]) also explore the pipeline of all-reduce communication tasks. Nevertheless, FFSMoE focuses more on inter- and intra-node communication overlaps within the MoE layer, while Lina only optimizes MoE-layer-specific communication bottlenecks and not the entire transformer block. Therefore, we aim to pipeline all major computing and communication tasks across the transformer block to minimize the per-iteration time, which involves three main challenges:

Complex dependencies between multi-type tasks. In distributed MoE training, there exists highly complex dependencies between the computing and communication tasks (see Figs. 2a and 2b) [10]. In particular, the typical parallelization schemes (e.g., pipeline parallelism [25, 26], tensor parallelism [27, 28, 29]) are difficult to be overlaid directly on expert parallelism.

Coexistence of A2A communication and all-reduce communication. Although there has been extensive studies [30, 16, 31, 15, 32, 33, 34] providing efficient scheduling algorithms for data-parallel training of all-reduce communication tasks, they focus on traditional convolution-based deep neural networks or LLMs without MoE layers. These studies cannot be directly applied to distributed MoE training because the additional A2A communication tasks are not equivalent to all-reduce communication tasks (see Fig. 2b).

Designing of an adaptive and generic pipeline scheduling framework. Currently, the performance of most scheduling frameworks depends on some hyperparameters setting [35, 36, 37], which introduces additional workload for tuning them before training. Ideally, an adaptive framework should automatically tune hyperparameters and be directly deployable by modifying only the model definition or dataset interface. Meanwhile, a general framework should also be designed to be compatible with different optimization frameworks and communication stacks.

In this paper, our main goal is to address the above three challenges by proposing a scalable pipeline scheduling framework called FlowMoE for multi-type tasks in distributed MoE training. All frequently used notations are summarized in Table A.1 of the Appendix.

3 FlowMoE

3.1 Overview

Fig. 3 illustrates the workflow of FlowMoE. FlowMoE performs efficient pipeline training leveraging the given MoE structure and the dataset. First, multi-type computing and communication tasks are broken down according to the pipelining degree and wait for pipeline scheduling. Second, FlowMoE schedules all computing and communication tasks according to their dependencies and defined priority for distributed training on the GPU cluster (see details in Secs. 3.2 and 3.3). Third, FlowMoE automatically tunes the partition size of all-reduce tensor based on the first several iterations during training by BO profiling (see details in Sec. 4.1).

3.2 Pipeline for MHA and MoE Layer

Based on the pipeline of the MoE layer, FlowMoE first pipelines the MHA layer computing and gating. It is worth noting that for the l th transformer block, the gating task only depends on the computing task of the MHA layer, and in the subsequent expression, we consider the computing task of both as a whole and denote it by $AT^{(l)}$ ($1 \leq l \leq L$). FlowMoE partitions the input tensor of each transformer block into R equal-sized parts, and each computing or communicating task (except all-reduce communicating task) in the MHA layer and the MoE layer will be partitioned into R independent subtasks. In particular, the tasks with the same type have the same execution time. The partitioned tasks can be represented as the set

$$\mathbb{T} = \left\{ AT_r^{(l)}, D_r^{(l)}, E_r^{(l)}, C_r^{(l)}, AR^{(l)} \mid 1 \leq r \leq R \right\}, \quad (1)$$

where $AT_r^{(l)}$ and $E_r^{(l)}$ are computing tasks, and $D_r^{(l)}$, $C_r^{(l)}$ and $AR^{(l)}$ are communication tasks.

Then, for $1 \leq l < L$, during feed-forward computing, the scheduling order of computing tasks can be denoted as

$$AT_1^{(l)} \rightarrow AT_2^{(l)} \rightarrow \dots \rightarrow AT_R^{(l)} \rightarrow E_1^{(l)} \rightarrow E_2^{(l)} \rightarrow \dots \rightarrow E_R^{(l)} \rightarrow AT_1^{(l+1)} \rightarrow \dots \rightarrow E_R^{(l+1)}, \quad (2)$$

the scheduling order of A2A communication tasks can be denoted as

$$D_1^{(l)} \rightarrow D_2^{(l)} \rightarrow \dots \rightarrow D_R^{(l)} \rightarrow C_1^{(l)} \rightarrow C_2^{(l)} \rightarrow \dots \rightarrow C_R^{(l)} \rightarrow D_1^{(l+1)} \rightarrow \dots \rightarrow C_R^{(l+1)}. \quad (3)$$

During backward propagation, the scheduling order of computing tasks can be denoted as

$$E_R^{(l+1)} \rightarrow \dots \rightarrow AT_1^{(l+1)} \rightarrow E_R^{(l)} \rightarrow E_{R-1}^{(l)} \rightarrow \dots \rightarrow E_1^{(l)} \rightarrow AT_R^{(l)} \rightarrow AT_{R-1}^{(l)} \rightarrow \dots \rightarrow AT_1^{(l)}, \quad (4)$$

the scheduling order of A2A communication tasks can be denoted as

$$C_R^{(l+1)} \rightarrow \dots \rightarrow D_1^{(l+1)} \rightarrow C_R^{(l)} \rightarrow C_{R-1}^{(l)} \rightarrow \dots \rightarrow C_1^{(l)} \rightarrow D_R^{(l)} \rightarrow D_{R-1}^{(l)} \rightarrow \dots \rightarrow D_1^{(l)}. \quad (5)$$

Figs. 2e and 2f show the example of execution timelines of the computing and communication tasks when pipelining the MHA layer and the MoE layer with $R = 2$. Compared to pipelining the MoE layer only, the MHA layer computing task and gating task can be overlapped with the A2A communication tasks, thus shortening the per-iteration time.

3.3 Pipeline for All-reduce Communication

Existing state-of-the-art scheduling frameworks centrally executes all-reduce communication tasks at the end of backward propagation for each iteration (we call it centralized scheduling of all-reduce communication tasks). To reduce all-reduce communication time, we further consider the pipeline of all-reduce communication tasks. Intuitively, in the backward propagation, the all-reduce communication task of transformer block l can overlap with computing tasks of transformer block $l - 1$, since they both depend on the completion of MHA layer computing tasks of transformer block l . However, in actual training, the all-reduce communication task of transformer block l will conflict with the A2A communication tasks of transformer block $l - 1$. Therefore, we first mathematically model the timeline of backward propagation in one iteration to find the optimal scheduling of the two communication tasks that minimizes the training time. Considering resource competition in real training environments, we assume that only computing and communication tasks can be executed simultaneously on a GPU, while multiple computing or multiple communication tasks cannot be run simultaneously. Furthermore, there is no preemption between tasks: once a task starts execution, it must run to completion without interruption. We define $\tau_b(\cdot)$ as the beginning execution timestamp of a task during the backward propagation, and $t_b(\cdot)$ as the elapsed time of a task during the backward propagation. According to Fig. 2b, the objective function and the dependencies between tasks can be expressed as follows ($1 \leq r \leq R$):

$$\min \quad T_b = \tau_b(AR^{(1)}) + t_b(AR^{(1)}) - \tau_b(C_R^{(L)}) \quad (6)$$

$$\text{s.t.} \quad \tau_b(C_r^{(l-1)}) \geq \tau_b(AT_r^{(l)}) + t_b(AT_r^{(l)}), 1 < l \leq L, \quad (6a)$$

$$\tau_b(E_r^{(l)}) \geq \tau_b(C_r^{(l)}) + t_b(C_r^{(l)}), 1 \leq l \leq L, \quad (6b)$$

$$\tau_b(D_r^{(l)}) \geq \tau_b(E_r^{(l)}) + t_b(E_r^{(l)}), 1 \leq l \leq L, \quad (6c)$$

$$\tau_b(AT_r^{(l)}) \geq \tau_b(D_r^{(l)}) + t_b(D_r^{(l)}), 1 \leq l \leq L, \quad (6d)$$

$$\tau_b(AR^{(l)}) \geq \tau_b(AT_r^{(l)}) + t_b(AT_r^{(l)}), 1 \leq l \leq L. \quad (6e)$$

We use the sign $*$ to denote the timeline for centralized scheduling of all-reduce communication tasks. Now, let T_b denote the backward propagation time when the all-reduce communication task of a transformer block is inserted between any two A2A communication tasks. Also denote by T_b^* the backward propagation time under centralized scheduling of all-reduce communication tasks. With this notation, we have the following theorem:

Theorem 1. *If the scheduling order satisfies Eqs. 4 and 5, then we have $T_b \leq T_b^*$.*

Proof. Theorem 1 proof is provided in Appendix B. \square

According to Theorem 1, we find that partitioning and inserting all-reduce communication tasks into the gaps between any of the A2A communication tasks can increase the overlap between all-reduce communication tasks and computing tasks. Thus, we design a priority scheduling mechanism of communication tasks based on the all-reduce tensor chunks in FlowMoE. Specifically, during the backward propagation, FlowMoE first slices the tensor for the all-reduce communication tasks of each layer into tensor chunks with size S_p . Second, FlowMoE maintains a communication task

Algorithm 1 Training process in FlowMoE

Input: Dataset $D = \{(x_1, y_1), \dots, (x_n, y_n)\}$, L .
Output: Model Weights $W = \{W_1, \dots, W_L\}$.

- 1: Initialize DataQueue for data transferred between tasks;
- 2: Initialize A2AQueue for A2A communication tasks;
- 3: Initialize ARQueue for all-reduce communication tasks;
- 4: Split D for d_1, d_2, \dots, d_R into DataQueue;
- 5: Communication_pool_management.start();
- 6: **for** $l = 1 \rightarrow L$ **do** //Feed-forward Computing
- 7: **for** $r = 1 \rightarrow R$ **do**
- 8: $d_r = \text{AT.FFcomp}(\text{DataQueue.get}())$;
- 9: A2AQueue.put(d_r);
- 10: **for** $r = 1 \rightarrow R$ **do**
- 11: $d_r = \text{E.FFcomp}(\text{DataQueue.get}())$;
- 12: A2AQueue.put(d_r);
- 13: **for** $l = L \rightarrow 1$ **do** //Backward Propagation
- 14: **for** $r = 1 \rightarrow R$ **do**
- 15: A2AQueue.put(d_r);
- 16: **for** $r = 1 \rightarrow R$ **do**
- 17: $d_r = \text{E.BPcomp}(\text{DataQueue.get}())$;
- 18: A2AQueue.put(d_r);
- 19: **for** $r = 1 \rightarrow R$ **do**
- 20: $d_r = \text{AT.BPcomp}(\text{DataQueue.get}())$;
- 21: DataQueue.put(d_r);
- 22: Waiting until all-reduce communication is finished;
- 23: Update W ;

Algorithm 2 Communication pool management

- 1: /* Partition an all-reduce tensor and enqueue tensor chunks. */
- 2: Get S_p from BO;
- 3: **procedure** PARTITION($ARTensor$)
- 4: $ARChunks = ARTensor.partition(S_p)$;
- 5: ARQueue.put($ARChunks$);
- 6: /* Communication task priority scheduling. */
- 7: **procedure** COMMPOOLMANAGER
- 8: **while** True **do**
- 9: **if** A2AQueue is not empty **then**
- 10: $d = \text{A2A.Comm}(\text{A2AQueue.get}())$;
- 11: DataQueue.put(d);
- 12: **else if** ARQueue is not empty **then**
- 13: $\text{AR.Comm}(\text{ARQueue.get}())$;

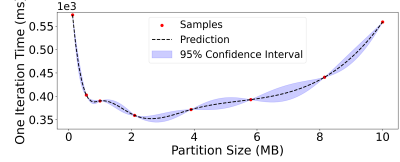


Figure 4: BO example: tuning S_p for training BERT-Large-MoE with a 16-GPU cluster.

pool which includes all the all-reduce tensor chunks and A2A communication tasks, and sets the scheduling priority of all-reduce tensor chunks to be lower than that of A2A communication tasks. In other words, the communication tasks of the all-reduce tensor chunks will be executed immediately when there is no A2A communication tasks. Fig. 2f shows an example of execution timeline when using 2-degree pipelining in MHA layer and MoE layer as well as priority scheduling mechanism of communication tasks based on all-reduce tensor chunks. It can be observed that the all-reduce tensor chunks fully occupy the gap between the A2A communication tasks and thereby maximize the overlap between the computing tasks and the communication tasks.

4 Parameter Optimization, Algorithm Design and System Implementation

4.1 Auto-Tuning Partition Size by Bayesian Optimization

Ideally, if the communication of all-reduce tensor chunks does not introduce extra startup overhead, we have the following theorem:

Theorem 2. *When the scheduling order satisfies Eqs. 4 and 5, and using the priority scheduling mechanism of communication tasks based on all-reduce tensor chunks, the time per iteration will be minimized if $S_p \rightarrow 0$ and there is no startup overhead for communicating all-reduce tensor chunks.*

Proof. Theorem 2 proof is provided in Appendix C. □

In the actual training, the communication tasks of all-reduce tensor chunks will introduce extra startup overhead [15]. Therefore, the partition size of all-reduce tensor chunks, S_p , becomes the knob that determines the trade-off between optimal scheduling and system overhead. Since it is non-trivial to explicitly model the iteration time as a function of S_p , to guarantee the adaptivity of FlowMoE, we adopt BO to automatically tune S_p during training, which attempts to find good parameters of an unknown objective function in as few number of trials as possible. BO's parameter settings, importance, and performance evaluation are described in detail in Appendix D. The goal of BO in FlowMoE is to minimize the per-iteration time. Specifically, BO fits an objective function by sampling different (S_p , per-iteration time) pairs and continuously suggests the next S_p to obtain a new objective function value, where the per-iteration time corresponding to different S_p in all pairs is measured from the average of multiple iterations (e.g., 10 iterations). In other words, BO can accurately predict a near-optimal S_p based on enough samples. Fig. 4 illustrates an example of using BO to tune S_p . In the actual training, with only 8 samples, BO returns a near-optimal value at 2.5MB with a good confidence.

Table 2: Benchmark models.

MoE Model	# Params (MHA+Gating)	# Params (Experts)	Dataset	Configurations							
				L	B	N	M	H	E/P	k	
GPT2-Tiny-MoE	3.2M	50.4M	OpenWebText	12	4	256	256	512	1	2	1.0
BERT-Large-MoE	25.2M	806.5M	wikitext-103	24	4	512	512	1024	2	1	1.0
LLaMA2-MoE	134.2M	4297.6M	wikitext-103	32	4	512	1024	4096	1	1	1.0
LLaMA2-MoE-L	268.4M	8595.2M	wikitext-103	64	4	512	1024	4096	1	1	1.0
DeepSeek-V2-S	419.6M	2014.1M	OpenWebText	4	4	256	5120	15362	8	1	1.0
DeepSeek-V2-M	734.3M	3524.7M	OpenWebText	7	4	256	5120	15362	1	1	1.0

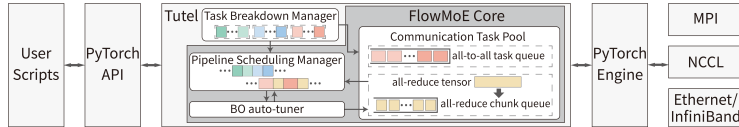


Figure 5: Overview of FlowMoE architecture (dark gray parts are new).

4.2 Algorithm Design

Algorithm 1 formally provides the pipeline scheduling training process of R -degree computing and communication tasks using FlowMoE. Moreover, Algorithm 2 provides the communication pool management, including the splitting of all-reduce tensors and the priority scheduling of communication tasks. A detailed description of the two algorithms is provided in Appendix E.

Compared to the vanilla expert parallelism [19], the overhead of pipeline scheduling in FlowMoE mainly comes from two parts: the partition of all-reduce tensors and the objective function fitting during BO. First, when the structure of the gating function is a typical linear layer of $M \times E$, the total number of parameters in the MHA layer and gating function is $4M^2 + M \times E$. According to Algorithm 2, the computational complexity of the scheduling algorithm of FlowMoE in each iteration is $\mathcal{O}(L \times \frac{4M^2 + M \times E}{S_p})$, which is acceptable because it is less than 1% of one iteration time in practical experiments, and the time of all-reduce tensor partitioning can be further overlapped with the time of some computing/communication tasks (we discuss its scalability in Appendix E).

Second, BO utilizes the first several iterations of the training process to automatically tune S_p to a near-optimal value. In our experiments, BO samples 8 values of S_p and record the iteration time corresponding to each value by averaging 10 iterations. The computational overhead introduced by BO is negligible compared to the total training time, as quantified in Appendix D. Additionally, if the hardware environment changes, BO will be re-executed to tune S_p , which is discussed in Appendix K. These details are omitted from the presentation of Algorithm 1 to focus more on the pipeline scheduling process of FlowMoE.

4.3 System Implementation

We deploy FlowMoE in PyTorch with its API, which usually supports class inheritance with flexible Python language and has a high generality to be compatible with different optimization frameworks and communication stacks. In particular, we implement FlowMoE atop Tutel [12], a highly optimized MoE acceleration library that is deeply integrated into PyTorch and supports asynchronous execution of communication and computing tasks. Tutel has also been used as a default MoE training module by DeepSpeed [38]. Fig. 5 shows the overview of FlowMoE architecture (the left side is closer to the user level), where its detailed description and technical implementations can be found in Appendix F.

5 Evaluation

5.1 Experimental Settings

Testbed setup. We use two clusters. (1) *Cluster 1* consists of 2 nodes connected with 100Gb/s bandwidth. Each node is equipped with 8 NVIDIA RTX3090 GPUs (24 GB of memory per GPU) connected with PCIe3.0x16. The CPU is Intel Xeon(R) Gold 6248R. (2) *Cluster 2* consists of 4 nodes connected with 10Gb/s bandwidth. Each node is equipped with 2 NVIDIA RTX2080Ti GPUs (12 GB of memory per GPU) connected with PCIe switches. The CPU is Intel Xeon(R) Gold 5118.

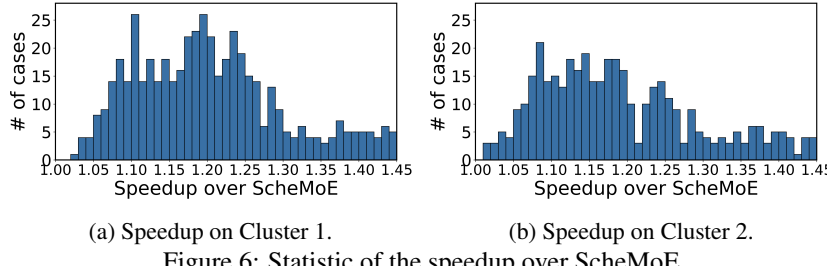
Models with MoE Layers. (1) *Customized MoE layers*: We cover typical configurations of MoE layers by choosing combinations of input parameters, where $B \in \{2, 4, 8\}$, $f \in \{1.0, 1.1, 1.2\}$, $N \in \{512, 1024, 2048\}$, $M \in \{512, 1024, 2048, 4096, 8192\}$ and $H \in \{512, 1024, 2048, 4096, 8192\}$.

Table 3: Comparison of average per-iteration time in milliseconds. S_1, S_2, S_3, S_4 and S_5 are the speedups of FlowMoE over ScheMoE, FSMoE, Tutel, FasterMoE, and vanillaEP, respectively.

# of GPUs	Model	Time (ms)						S_5	S_4	S_3	S_2	S_1
		vanillaEP	FasterMoE	Tutel	FSMoE	ScheMoE	FlowMoE					
4	GPT2-Tiny-MoE	104.2	90.1	85.6	82.8	80.8	66.1	$1.58 \times 1.36 \times 1.29 \times 1.25 \times 1.22 \times$				
	BERT-Large-MoE	373.1	300.9	314.6	278.1	273.6	239.5	$1.56 \times 1.26 \times 1.31 \times 1.16 \times 1.14 \times$				
	LLaMA2-MoE	1262.3	1187.5	1029.5	928.1	957.7	763.9	$1.65 \times 1.55 \times 1.34 \times 1.21 \times 1.25 \times$				
	DeepSeek-V2-S	2789.7	2261.4	2276.5	2096.3	2166.1	1740.8	$1.60 \times 1.29 \times 1.30 \times 1.20 \times 1.24 \times$				
8	GPT2-Tiny-MoE	125.1	119.3	116.8	98.8	107.5	87.6	$1.43 \times 1.36 \times 1.33 \times 1.13 \times 1.23 \times$				
	BERT-Large-MoE	428.8	354.4	377.5	345.1	331.2	283.2	$1.51 \times 1.25 \times 1.33 \times 1.22 \times 1.17 \times$				
	LLaMA2-MoE	1563.3	1427.7	1187.9	1110.4	1089.9	906.0	$1.73 \times 1.57 \times 1.31 \times 1.23 \times 1.20 \times$				
	DeepSeek-V2-S	4037.8	3370.5	3351.7	2985.4	3138.3	2384.9	$1.69 \times 1.41 \times 1.39 \times 1.25 \times 1.31 \times$				
16	GPT2-Tiny-MoE	169.5	135.3	129.3	114.8	116.4	95.6	$1.77 \times 1.41 \times 1.35 \times 1.20 \times 1.22 \times$				
	BERT-Large-MoE	537.8	490.8	501.1	421.9	405.6	351.9	$1.53 \times 1.39 \times 1.42 \times 1.19 \times 1.15 \times$				
	LLaMA2-MoE	1987.7	1759.1	1534.1	1292.6	1374.3	1124.0	$1.76 \times 1.57 \times 1.36 \times 1.15 \times 1.22 \times$				
	DeepSeek-V2-S	5843.3	4562.5	4481.4	3895.6	4093.7	3205.3	$1.82 \times 1.42 \times 1.39 \times 1.22 \times 1.28 \times$				

Table 4: Average per-iteration time with different pipelining degrees on DeepSeek-V2-S. S_1 and S_2 are the speedups of FlowMoE over Tutel and ScheMoE, respectively.

R	Time (ms)			S_2	S_1
	Tutel	ScheMoE	FlowMoE		
2	4481.4	4093.7	3205.3	$1.39 \times$	$1.28 \times$
4	4628.2	4164.0	3113.8	$1.48 \times$	$1.33 \times$
8	4588.9	4308.7	3295.9	$1.39 \times$	$1.30 \times$



(a) Speedup on Cluster 1.

(b) Speedup on Cluster 2.

Figure 6: Statistic of the speedup over ScheMoE.

We set the number of experts equal to the number of GPUs (i.e., $E = P$) and $k = 2$. (2) *Real-world MoE models*: We also choose four popular models, i.e., GPT2-Tiny-MoE and DeepSeek-V2 [39] for the language modeling task on the OpenWebText dataset [40], and BERT-Large-MoE and LLaMA2-MoE for the text generation task on the wikitext-103 dataset [41]. We replace all feed-forward layers in GPT2-Tiny [42], BERT-Large [43], and LLaMA2 [44] with MoE layers to construct MoE models. The detailed configuration is shown in Table 2. All parameters and gradients of MoE models are stored as 32-bit single precision floating point numbers.

Baselines. We compare FlowMoE with PyTorch-based vanilla expert parallelism (vanillaEP) [19] and existing state-of-the-art MoE frameworks, including ScheMoE [10], FSMoE [24], Tutel [12] and FasterMoE [11], with a pipelining degree of $R = 2$ unless specified otherwise. We use the official implementations of these frameworks. We focus on per-iteration training time, energy consumption and memory usage as performance metrics. All the reported numbers are averaged over 1000 iterations.

5.2 Experimental Results

End-to-end Time on Real-world MoE Models. We measure the average iteration time for end-to-end training of the models listed in Table 2 on Cluster 1. The experimental results are shown in Table 3. The results show that FlowMoE obtains the best scalability and the shortest per-iteration time on different sizes of clusters and models. Specifically, FlowMoE is 14%-31%, 13%-25%, 29%-42%, 26%-57% and 43%-82% faster than ScheMoE, FSMoE, Tutel, FasterMoE and vanillaEP, respectively.

Table 5: Per-iteration time of the MoE layer under different components. The reported speedup values are based on vanillaEP as the baseline. ‘w/ Pipe-MoE’ indicates pipelining expert computing and A2A communication. ‘w/ Pipe-AT’ indicates pipelining MHA layer computing and gating. ‘w/ Pipe-AR’ indicates pipelining all-reduce communication.

Name	w/ Pipe-MoE	w/ Pipe-AT	w/ Pipe-AR	Time (ms)	Speedup
vanillaEP	×	×	×	1630.8	1.0×
Tutel	√	×	×	1115.2	1.46×
FlowMoE-AT	√	√	×	1012.6	1.61×
FlowMoE-AR	√	×	√ (w/o BO)	971.5	1.68×
FlowMoE-AR(BO)	√	×	√ (w/ BO)	895.3	1.82×
FlowMoE	√	√	√	796.1	2.05×

We also execute stress tests on different training frameworks across two scaled-up MoE models (LLaMA2-MoE-L and DeepSeek-V2-M) in Appendix G. Moreover, in most cases, Tutel is faster than FasterMoE due to its dedicated optimization for MoE training. Both FlowMoE and ScheMoE are built atop Tutel and outperform Tutel. ScheMoE and FSMoE further reduce training time by optimizing scheduling within the MoE layer and pipelining intra- and inter-node communication tasks, and this strategy can also be integrated into FlowMoE. In contrast, our proposed FlowMoE maximally overlaps communication with computing by pipelining all types of tasks. In bandwidth-limited scenarios, when the number of GPUs scales up, pipeline scheduling benefits less and longer communication time dominates the whole training process, thus the advantages of FlowMoE and other state-of-the-art MoE frameworks are not obvious. Moreover, FlowMoE essentially only changes the scheduling order of different tasks and does not affect the model convergence. We verify it through theoretical analysis and practical convergence experiments in Appendix H. Furthermore, we discuss the performance lower bound of FlowMoE in Appendix I and report the GPU SM utilization when training with FlowMoE in detail in Appendix J. We evaluate the sensitivity of FlowMoE to S_p selection and BO hyperparameters, while measure the computational overhead of BO in Appendix D. We also discuss the robustness of FlowMoE to heterogeneous clusters, dynamic hardware environments, and node dropouts in Appendix K.

Pipelining degree v.s. Training Speed. Table 4 presents the averaged iteration time with different R values on Cluster 1 with 16 GPUs. FlowMoE consistently outperforms ScheMoE and Tutel. Prior work [21] has provided an effective method to select the optimal R by balancing overlapping degree and startup overhead of the tasks, which can be directly applied to FlowMoE. Orthogonal to the methods in choosing the best R , our scheduling framework focuses on pipelining all computing and communication tasks efficiently for any given $R \geq 2$.

Speedup on Customized MoE Layers. We construct the MoE layer using a combination of input parameters from customized MoE layer. We collect 490 valid cases from Cluster 1 with 16 GPUs and 393 cases from Cluster 2 with 8 GPUs (excluding out-of-memory cases) successfully measured on ScheMoE and FlowMoE, respectively. FlowMoE is always faster than ScheMoE in all valid cases. The speedup statistic of FlowMoE over ScheMoE is shown in Fig. 6. On average, FlowMoE achieves 26% improvement over ScheMoE.

Ablation Study. We conduct the ablation study on a customized MoE layer with $B = 4$, $f = 1.2$, $N = 512$, $M = 8192$, and $H = 8192$. The per-iteration time on Cluster 1 with different components using 16 GPUs is shown in Table 4. It is seen that FlowMoE-AT improve the time performance by 10.3% over Tutel by pipelining the MHA layer computing and gating. Further, FlowMoE-AR(BO) utilizes the priority scheduling mechanism of communication tasks based on all-reduce tensor chunks to pipeline the all-reduce communication and improve the time performance by another 24.6% over Tutel. In particular, our designed BO finds the near-optimal S_p and FlowMoE-AR(BO) obtains 8.3% improvement in training time compared to FlowMoE-AR (where we set $S_p = 1\text{MB}$). Putting our two optimizations together, FlowMoE runs 1.4× and 2.05× faster than Tutel and vanillaEP, respectively.

Energy Consumption. We use the NVIDIA SMI tool to sample the real-time power of each GPU in the cluster every 5ms, then integrate these sampled data over time to calculate the energy consumption of each GPU during the training process. We sum the energy consumption of all GPUs to obtain the total energy consumption, then divide it by the number of GPUs and the number of iterations to obtain the average per-worker energy consumption as shown in Table 6. The results indicate that a higher overlapping degree of computing and communication tasks leads to higher computing and

Table 6: Averaged per-worker energy consumption and memory usage in one iteration.

Model	vanillaEP	FasterMoE	Tutel	ScheMoE	FlowMoE
GPT2-Tiny-MoE	1.7J/2.45GB	1.5J/2.67GB	1.3J/2.52GB	1.2J/2.46GB	1.0J/2.42GB
BERT-Large-MoE	5.5J/4.19GB	5.9J/4.97GB	5.1J/4.13GB	4.1J/4.16GB	3.7J/3.89GB
LLaMA2-MoE	20.2J/12.43GB	19.9J/16.11GB	15.6J/11.59GB	14.0J/11.81GB	12.1J/11.01GB
DeepSeek-V2-S	59.5J/19.42GB	54.9J/20.93GB	45.6J/19.34GB	41.7J/18.92GB	34.9J/17.57GB

communication resource utilization, thus exhibiting lower energy consumption. Overall, FlowMoE saves 10%-16%, 22%-27%, 33%-39% and 33%-41% energy consumption compared to ScheMoE, Tutel, FasterMoE and vanillaEP, respectively. It is worth noting that the power reported by the NVIDIA SMI tool includes both communication and computing costs. According to the official documentation of NVIDIA SMI [45], the energy consumption measured by the NVIDIA SMI tool covers the entire GPU card’s power consumption, where communication power includes (1) PCIe communication costs, (2) NVLink/NVSwitch communication costs, and (3) collective communication costs (e.g., NCCL All-Reduce and A2A). Therefore, our measurement results effectively reflect the total cluster-wide energy usage, compatibly providing a fair comparison with the baselines.

Memory Usage. Table 6 also demonstrates average memory usage per worker by monitoring all GPUs every 1s on Cluster 1 with 16 GPUs using the NVIDIA SMI tool. FlowMoE has the lowest memory usage because it performs all-reduce communication tasks in time to reduce gradient caching. Specifically, FlowMoE saves up to 7%, 9%, 32% and 11% of memory compared to ScheMoE, Tutel, FasterMoE and vanillaEP, respectively. In addition, the memory usage of ScheMoE and Tutel is similar to that of vanillaEP since there is no optimization in the memory. FasterMoE needs to replicate expert parameters among workers in its load balancing mechanism and consumes more GPU memory.

6 Related Work

In addition to the frameworks mentioned in Section 2 that focus on computing-communication pipelines in distributed training, we also discuss some other works. First, general pipeline schedulers such as PipeDream [26] and Gpipe [25] enable pipelining by splitting the model across multiple GPUs, requiring communication between GPUs to exchange activation values or gradients across split layers. In contrast, FlowMoE implements pipelining of computing-communication tasks, accelerating model training by minimizing communication overhead. Second, several orthogonal MoE optimization techniques can be combined with FlowMoE. (1) NetMoE [46] alleviates communication bottlenecks and load imbalance by reducing cross-node token routing and dynamically adjusting expert placement. (2) Lancet [47] determines task scheduling order by constructing a computing-communication directed acyclic graph (DAG), without considering microbatch-level partitioning of the same task. (3) Punniyamurthy et al.’s work [48] focuses on fusing computing-communication operations and reducing kernel-level startup overhead. However, it does not consider scheduling relationships among all major MoE tasks or how to maximize computing-communication overlap.

7 Conclusion

In this paper, we propose a scalable and mathematically proven pipeline scheduling framework called FlowMoE to accelerate the training of MoE models. FlowMoE addresses the unified scheduling across all major MoE-related tasks and enables the optimal coexistence of heterogeneous communication tasks (A2A and all-reduce communications) in MoE training. This substantially advances distributed solutions beyond a simple extension of traditional pipeline methods. We implement the FlowMoE framework on Pytorch. We conduct extensive experiments with 675 typical MoE layers and four real-world NLP models across two GPU clusters. Experimental results show that FlowMoE outperforms state-of-the-art MoE training frameworks including ScheMoE, FFSMoE, Tutel, and FasterMoE by 13%-57% in training time, 10%-39% in energy consumption, and 7%-32% in memory usage. Furthermore, FlowMoE can be combined with many orthogonal optimization works, promoting distributed pipeline optimization to a new stage.

8 Acknowledgements

This work was supported in part by the National Key Research and Development Project under Grant 2022YFB2901604.

References

- [1] Tom Brown, Benjamin Mann, Nick Ryder, Melanie Subbiah, Jared D Kaplan, Prafulla Dhariwal, Arvind Neelakantan, Pranav Shyam, Girish Sastry, Amanda Askell, et al. Language Models are Few-Shot Learners. In *Advances in Neural Information Processing Systems*, volume 33, pages 1877–1901, 2020.
- [2] Abhimanyu Dubey, Abhinav Jauhri, Abhinav Pandey, Abhishek Kadian, Ahmad Al-Dahle, Aiesha Letman, Akhil Mathur, Alan Schelten, Amy Yang, Angela Fan, et al. The Llama 3 Herd of Models. *arXiv preprint arXiv:2407.21783*, 2024.
- [3] Daya Guo, Dejian Yang, Haowei Zhang, Junxiao Song, Ruoyu Zhang, Runxin Xu, Qihao Zhu, Shirong Ma, Peiyi Wang, Xiao Bi, et al. DeepSeek-R1: Incentivizing Reasoning Capability in LLMs via Reinforcement Learning. *arXiv preprint arXiv:2501.12948*, 2025.
- [4] Robert A Jacobs, Michael I Jordan, Steven J Nowlan, and Geoffrey E Hinton. Adaptive Mixtures of Local Experts. *Neural Computation*, 3(1):79–87, 1991.
- [5] Dmitry Lepikhin, HyoukJoong Lee, Yuanzhong Xu, Dehao Chen, Orhan Firat, Yanping Huang, Maxim Krikun, Noam Shazeer, and Zhipeng Chen. GShard: Scaling Giant Models with Conditional Computation and Automatic Sharding. *arXiv preprint arXiv:2006.16668*, 2020.
- [6] Noam Shazeer, Azalia Mirhoseini, Krzysztof Maziarz, Andy Davis, Quoc Le, Geoffrey Hinton, and Jeff Dean. Outrageously Large Neural Networks: The Sparsely-Gated Mixture-of-Experts Layer. *arXiv preprint arXiv:1701.06538*, 2017.
- [7] Zixuan Ma, Jiaao He, Jiezhong Qiu, Huanqi Cao, Yuanwei Wang, Zhenbo Sun, Liyan Zheng, Haojie Wang, Shizhi Tang, Tianyu Zheng, et al. BaGuLu: Targeting Brain Scale Pretrained Models with over 37 Million Cores. In *Proceedings of the 27th ACM SIGPLAN Symposium on Principles and Practice of Parallel Programming*, pages 192–204, 2022.
- [8] Carlos Riquelme, Joan Puigcerver, Basil Mustafa, Maxim Neumann, Rodolphe Jenatton, André Susano Pinto, Daniel Keysers, and Neil Houlsby. Scaling Vision with Sparse Mixture of Experts. In *Advances in Neural Information Processing Systems*, volume 34, pages 8583–8595, 2021.
- [9] William Fedus, Barret Zoph, and Noam Shazeer. Switch Transformers: Scaling to Trillion Parameter Models with Simple and Efficient Sparsity. *Journal of Machine Learning Research*, 23(120):1–39, 2022.
- [10] Shaohuai Shi, Xinglin Pan, Qiang Wang, Chengjian Liu, Xiaozhe Ren, Zhongzhe Hu, Yu Yang, Bo Li, and Xiaowen Chu. ScheMoE: An Extensible Mixture-of-Experts Distributed Training System with Tasks Scheduling. In *Proceedings of the 19th European Conference on Computer Systems*, pages 236–249, 2024.
- [11] Jiaao He, Jidong Zhai, Tiago Antunes, Haojie Wang, Fuwen Luo, Shangfeng Shi, and Qin Li. FasterMoE: Modeling and Optimizing Training of Large-Scale Dynamic Pre-Trained Models. In *Proceedings of the 27th ACM SIGPLAN Symposium on Principles and Practice of Parallel Programming*, pages 120–134, 2022.
- [12] Changho Hwang, Wei Cui, Yifan Xiong, Ziyue Yang, Ze Liu, Han Hu, Zilong Wang, Rafael Salas, Jithin Jose, Prabhat Ram, et al. Tutel: Adaptive Mixture-of-Experts at Scale. In *Proceedings of Machine Learning and Systems*, volume 5, pages 269–287, 2023.
- [13] Jehoshua Bruck, Ching-Tien Ho, Shlomo Kipnis, and Derrick Weathersby. Efficient Algorithms for All-to-All Communications in Multi-Port Message-Passing Systems. In *Proceedings of the 6th Annual ACM Symposium on Parallel Algorithms and Architectures*, pages 298–309, 1994.
- [14] Jeffrey Dean, Greg Corrado, Rajat Monga, Kai Chen, Matthieu Devin, Mark Mao, Marc’ aurelio Ranzato, Andrew Senior, Paul Tucker, Ke Yang, et al. Large Scale Distributed Deep Networks. In *Advances in Neural Information Processing Systems*, volume 25, 2012.
- [15] Yunqi Gao, Bing Hu, Mahdi Boloursaz Mashhadi, A-Long Jin, Pei Xiao, and Chunming Wu. US-Byte: An Efficient Communication Framework for Scheduling Unequal-Sized Tensor Blocks in Distributed Deep Learning. *IEEE Transactions on Parallel and Distributed Systems*, 35(1):123–139, 2023.

[16] Shaohuai Shi, Xiaowen Chu, and Bo Li. MG-WFBP: Efficient Data Communication for Distributed Synchronous SGD Algorithms. In *IEEE INFOCOM 2019-IEEE Conference on Computer Communications*, pages 172–180, 2019.

[17] Xianyan Jia, Shutao Song, Wei He, Yangzihao Wang, Haidong Rong, Feihu Zhou, Liqiang Xie, Zhenyu Guo, Yuanzhou Yang, Liwei Yu, et al. Highly Scalable Deep Learning Training System with Mixed-Precision: Training ImageNet in Four Minutes. *arXiv preprint arXiv:1807.11205*, 2018.

[18] Yang You, Jing Li, Sashank J. Reddi, Jonathan Hseu, Sanjiv Kumar, Srinadh Bhojanapalli, Xiaodan Song, James Demmel, Kurt Keutzer, and Cho-Jui Hsieh. Large Batch Optimization for Deep Learning: Training BERT in 76 minutes. In *8th International Conference on Learning Representations, ICLR 2020, Addis Ababa, Ethiopia, April 26-30, 2020*, 2020.

[19] Jiaao He, Jiezhong Qiu, Aohan Zeng, Zhilin Yang, Jidong Zhai, and Jie Tang. FastMoE: A Fast Mixture-of-Expert Training System. *arXiv preprint arXiv:2103.13262*, 2021.

[20] Jiamin Li, Yimin Jiang, Yibo Zhu, Cong Wang, and Hong Xu. Accelerating Distributed MoE Training and Inference with Lina. In *2023 USENIX Annual Technical Conference (USENIX ATC 23)*, pages 945–959, 2023.

[21] Shaohuai Shi, Xinglin Pan, Xiaowen Chu, and Bo Li. PipeMoE: Accelerating Mixture-of-Experts through Adaptive Pipelining. In *IEEE INFOCOM 2023-IEEE Conference on Computer Communications*, pages 1–10, 2023.

[22] Shulai Zhang, Ningxin Zheng, Haibin Lin, Ziheng Jiang, Wenlei Bao, Chengquan Jiang, Qi Hou, Weihao Cui, Size Zheng, and et al. Chang, Li-Wen. Comet: Fine-grained computation-communication overlapping for mixture-of-experts. *arXiv preprint arXiv:2502.19811*, 2025.

[23] Adam Paszke, Sam Gross, Francisco Massa, Adam Lerer, James Bradbury, Gregory Chanan, Trevor Killeen, Zeming Lin, Natalia Gimelshein, Luca Antiga, et al. PyTorch: An Imperative Style, High-Performance Deep Learning Library. *Advances in Neural Information Processing Systems*, 32, 2019.

[24] Xinglin Pan, Wenxiang Lin, Lin Zhang, Shaohuai Shi, Zhenheng Tang, Rui Wang, Bo Li, and Xiaowen Chu. FSMoE: A Flexible and Scalable Training System for Sparse Mixture-of-Experts Models. In *Proceedings of the 30th ACM International Conference on Architectural Support for Programming Languages and Operating Systems, Volume 1*, page 524–539, 2025.

[25] Yanping Huang, Youlong Cheng, Ankur Bapna, Orhan Firat, Dehao Chen, Mia Chen, HyoukJoong Lee, Jiquan Ngiam, Quoc V Le, Yonghui Wu, et al. GPipe: Efficient Training of Giant Neural Networks using Pipeline Parallelism. *Advances in Neural Information Processing Systems*, 32, 2019.

[26] Deepak Narayanan, Aaron Harlap, Amar Phanishayee, Vivek Seshadri, Nikhil R Devanur, Gregory R Ganger, Phillip B Gibbons, and Matei Zaharia. PipeDream: Generalized Pipeline Parallelism for DNN Training. In *Proceedings of the 27th ACM Symposium on Operating Systems Principles*, pages 1–15, 2019.

[27] Lianmin Zheng, Zhuohan Li, Hao Zhang, Yonghao Zhuang, Zhifeng Chen, Yanping Huang, Yida Wang, Yuanzhong Xu, Danyang Zhuo, Eric P Xing, et al. Alpa: Automating Inter- and Intra-Operator Parallelism for Distributed Deep Learning. In *16th USENIX Symposium on Operating Systems Design and Implementation (OSDI 22)*, pages 559–578, 2022.

[28] Mohammad Shoeybi, Mostofa Patwary, Raul Puri, Patrick LeGresley, Jared Casper, and Bryan Catanzaro. Megatron-LM: Training Multi-Billion Parameter Language Models Using Model Parallelism. *arXiv preprint arXiv:1909.08053*, 2019.

[29] Mingshu Zhai, Jiaao He, Zixuan Ma, Zan Zong, Runqing Zhang, and Jidong Zhai. SmartMoE: Efficiently Training Sparsely-Activated Models through Combining Offline and Online Parallelization. In *2023 USENIX Annual Technical Conference (USENIX ATC 23)*, pages 961–975, 2023.

[30] Hao Zhang, Zeyu Zheng, Shizhen Xu, Wei Dai, Qirong Ho, Xiaodan Liang, Zhiting Hu, Jinliang Wei, Pengtao Xie, and Eric P Xing. Poseidon: An Efficient Communication Architecture for Distributed Deep Learning on GPU Clusters. In *2017 USENIX Annual Technical Conference (USENIX ATC 17)*, pages 181–193, 2017.

[31] Yanghua Peng, Yibo Zhu, Yangrui Chen, Yixin Bao, Bairen Yi, Chang Lan, Chuan Wu, and Chuanxiong Guo. A Generic Communication Scheduler for Distributed DNN Training Acceleration. In *Proceedings of the 27th ACM Symposium on Operating Systems Principles*, pages 16–29, 2019.

[32] Chang Chen, Xiuhong Li, Qianchao Zhu, Jiangfei Duan, Peng Sun, Xingcheng Zhang, and Chao Yang. Centauri: Enabling efficient scheduling for communication-computation overlap in large model training via communication partitioning. In *Proceedings of the 29th ACM International Conference on Architectural Support for Programming Languages and Operating Systems, Volume 3*, pages 178–191, 2024.

[33] Abhinav Jangda, Jun Huang, Guodong Liu, Amir Hossein Nodehi Sabet, Saeed Maleki, Youshan Miao, Madanlal Musuvathi, Todd Mytkowicz, and Olli Saarikivi. Breaking the computation and communication abstraction barrier in distributed machine learning workloads. In *Proceedings of the 27th ACM International Conference on Architectural Support for Programming Languages and Operating Systems*, pages 402–416, 2022.

[34] Shibo Wang, Jinliang Wei, Amit Sabne, Andy Davis, Berkin Ilbeyi, Blake Hechtman, Dehao Chen, Karthik Srinivasa Murthy, Marcello Maggioni, Qiao Zhang, et al. Overlap communication with dependent computation via decomposition in large deep learning models. In *Proceedings of the 28th ACM International Conference on Architectural Support for Programming Languages and Operating Systems, Volume 1*, pages 93–106, 2022.

[35] Yixin Bao, Yanghua Peng, Yangrui Chen, and Chuan Wu. Preemptive All-reduce Scheduling for Expediting Distributed DNN Training. In *IEEE INFOCOM 2020-IEEE Conference on Computer Communications*, pages 626–635, 2020.

[36] Shaohuai Shi, Xiaowen Chu, and Bo Li. Exploiting Simultaneous Communications to Accelerate Data Parallel Distributed Deep Learning. In *IEEE INFOCOM 2021-IEEE Conference on Computer Communications*, pages 1–10, 2021.

[37] Yunqi Gao, Bing Hu, Mahdi Boloursaz Mashhadi, Wei Wang, Rahim Tafazolli, and Merouane Debbah. A Dynamic Sliding Window Based Tensor Communication Scheduling Framework for Distributed Deep Learning. *IEEE Transactions on Network Science and Engineering*, 12(2):1080–1095, 2024.

[38] Samyam Rajbhandari, Conglong Li, Zhewei Yao, Minjia Zhang, Reza Yazdani Aminabadi, Ammar Ahmad Awan, Jeff Rasley, and Yuxiong He. DeepSpeed-MoE: Advancing Mixture-of-Experts Inference and Training to Power Next-Generation AI Scale. In *International Conference on Machine Learning*, pages 18332–18346, 2022.

[39] Aixin Liu, Bei Feng, Bin Wang, Bingxuan Wang, Bo Liu, Chenggang Zhao, Chengqi Deng, Chong Ruan, Damai Dai, Daya Guo, et al. DeepSeek-V2: A Strong, Economical, and Efficient Mixture-of-Experts Language Model. *arXiv preprint arXiv:2405.04434*, 2024.

[40] Stephen Merity, Caiming Xiong, James Bradbury, Joshua Socher, Richard Peterson, Stephan Meylan, and David Bourgin. Openwebtext dataset. <https://github.com/jcpeterson/openwebtext>, 2019.

[41] Stephen Merity, Caiming Xiong, James Bradbury, and Richard Socher. Pointer Sentinel Mixture Models. *arXiv preprint arXiv:1609.07843*, 2016.

[42] Alec Radford, Jeffrey Wu, Rewon Child, David Luan, Dario Amodei, Ilya Sutskever, et al. Language Models are Unsupervised Multitask Learners. *OpenAI blog*, 1(8):9, 2019.

[43] Jacob Devlin, Ming-Wei Chang, Kenton Lee, and Kristina Toutanova. BERT: Pre-training of Deep Bidirectional Transformers for Language Understanding. In *Proceedings of the 2019 Conference of the North American Chapter of the Association for Computational Linguistics: Human Language Technologies, Volume 1 (Long and Short Papers)*, pages 4171–4186, 2019.

[44] Hugo Touvron, Louis Martin, Kevin Stone, Peter Albert, Amjad Almahairi, Yasmine Babaei, Nikolay Bashlykov, Soumya Batra, Prajjwal Bhargava, Shruti Bhosale, et al. Llama 2: Open Foundation and Fine-Tuned Chat Models. *arXiv preprint arXiv:2307.09288*, 2023.

[45] NVIDIA Corporation. *NVIDIA System Management Interface (nvidia-smi) User Guide*, 2025. URL <https://developer.nvidia.com/system-management-interface>.

[46] Xinyi Liu, Yujie Wang, Fangcheng Fu, Xupeng Miao, Shenhan Zhu, Xiaonan Nie, and Bin Cui. Netmoe: Accelerating moe training through dynamic sample placement. In *The Thirteenth International Conference on Learning Representations*, 2025.

[47] Chenyu Jiang, Ye Tian, Zhen Jia, Shuai Zheng, Chuan Wu, and Yida Wang. Lancet: Accelerating mixture-of-experts training via whole graph computation-communication overlapping. In *Proceedings of Machine Learning and Systems*, volume 6, pages 74–86, 2024.

[48] Kishore Punniyamurthy, Khaled Hamidouche, and Bradford M Beckmann. Optimizing distributed ml communication with fused computation-collective operations. In *SC24: International Conference for High Performance Computing, Networking, Storage and Analysis*, pages 1–17, 2024.

[49] Omid Alipourfard, Hongqiang Harry Liu, Jianshu Chen, Shivaram Venkataraman, Minlan Yu, and Ming Zhang. CherryPick: Adaptively Unearthing the Best Cloud Configurations for Big Data Analytics. In *14th USENIX Symposium on Networked Systems Design and Implementation, NSDI*, pages 469–482, 2017.

[50] Lin Zhang, Shaohuai Shi, Xiaowen Chu, Wei Wang, Bo Li, and Chengjian Liu. DeAR: Accelerating Distributed Deep Learning with Fine-Grained All-Reduce Pipelining. In *IEEE 43rd International Conference on Distributed Computing Systems (ICDCS)*, pages 142–153, 2023.

[51] Richard L Graham, Timothy S Woodall, and Jeffrey M Squyres. Open MPI: A Flexible High Performance MPI. In *Parallel Processing and Applied Mathematics: 6th International Conference, PPAM 2005, Poznań, Poland, September 11-14, 2005, Revised Selected Papers 6*, pages 228–239, 2006.

[52] Min Si, Yutaka Ishikawa, and Masamichi Tatagi. Direct MPI Library for Intel Xeon Phi Co-Processors. In *2013 IEEE International Symposium on Parallel & Distributed Processing, Workshops and Phd Forum*, pages 816–824, 2013.

NeurIPS Paper Checklist

1. Claims

Question: Do the main claims made in the abstract and introduction accurately reflect the paper's contributions and scope?

Answer: [\[Yes\]](#)

Justification: We describe our scope and contributions in the abstract and introduction.

Guidelines:

- The answer NA means that the abstract and introduction do not include the claims made in the paper.
- The abstract and/or introduction should clearly state the claims made, including the contributions made in the paper and important assumptions and limitations. A No or NA answer to this question will not be perceived well by the reviewers.
- The claims made should match theoretical and experimental results, and reflect how much the results can be expected to generalize to other settings.
- It is fine to include aspirational goals as motivation as long as it is clear that these goals are not attained by the paper.

2. Limitations

Question: Does the paper discuss the limitations of the work performed by the authors?

Answer: [\[Yes\]](#)

Justification: We analyze the limitations of our approach based on the experimental results in Section 5.2.

Guidelines:

- The answer NA means that the paper has no limitation while the answer No means that the paper has limitations, but those are not discussed in the paper.
- The authors are encouraged to create a separate "Limitations" section in their paper.
- The paper should point out any strong assumptions and how robust the results are to violations of these assumptions (e.g., independence assumptions, noiseless settings, model well-specification, asymptotic approximations only holding locally). The authors should reflect on how these assumptions might be violated in practice and what the implications would be.
- The authors should reflect on the scope of the claims made, e.g., if the approach was only tested on a few datasets or with a few runs. In general, empirical results often depend on implicit assumptions, which should be articulated.
- The authors should reflect on the factors that influence the performance of the approach. For example, a facial recognition algorithm may perform poorly when image resolution is low or images are taken in low lighting. Or a speech-to-text system might not be used reliably to provide closed captions for online lectures because it fails to handle technical jargon.
- The authors should discuss the computational efficiency of the proposed algorithms and how they scale with dataset size.
- If applicable, the authors should discuss possible limitations of their approach to address problems of privacy and fairness.
- While the authors might fear that complete honesty about limitations might be used by reviewers as grounds for rejection, a worse outcome might be that reviewers discover limitations that aren't acknowledged in the paper. The authors should use their best judgment and recognize that individual actions in favor of transparency play an important role in developing norms that preserve the integrity of the community. Reviewers will be specifically instructed to not penalize honesty concerning limitations.

3. Theory assumptions and proofs

Question: For each theoretical result, does the paper provide the full set of assumptions and a complete (and correct) proof?

Answer: [\[Yes\]](#)

Justification: We describe the theory assumptions and proofs in Section 3.3, Section 4.1, Appendix B and Appendix C.

Guidelines:

- The answer NA means that the paper does not include theoretical results.
- All the theorems, formulas, and proofs in the paper should be numbered and cross-referenced.
- All assumptions should be clearly stated or referenced in the statement of any theorems.
- The proofs can either appear in the main paper or the supplemental material, but if they appear in the supplemental material, the authors are encouraged to provide a short proof sketch to provide intuition.
- Inversely, any informal proof provided in the core of the paper should be complemented by formal proofs provided in appendix or supplemental material.
- Theorems and Lemmas that the proof relies upon should be properly referenced.

4. Experimental result reproducibility

Question: Does the paper fully disclose all the information needed to reproduce the main experimental results of the paper to the extent that it affects the main claims and/or conclusions of the paper (regardless of whether the code and data are provided or not)?

Answer: [\[Yes\]](#)

Justification: We clearly and fully present the selected models and benchmarks in Section 5 and also describe some parameter settings in Appendix D.1.

Guidelines:

- The answer NA means that the paper does not include experiments.
- If the paper includes experiments, a No answer to this question will not be perceived well by the reviewers: Making the paper reproducible is important, regardless of whether the code and data are provided or not.
- If the contribution is a dataset and/or model, the authors should describe the steps taken to make their results reproducible or verifiable.
- Depending on the contribution, reproducibility can be accomplished in various ways. For example, if the contribution is a novel architecture, describing the architecture fully might suffice, or if the contribution is a specific model and empirical evaluation, it may be necessary to either make it possible for others to replicate the model with the same dataset, or provide access to the model. In general, releasing code and data is often one good way to accomplish this, but reproducibility can also be provided via detailed instructions for how to replicate the results, access to a hosted model (e.g., in the case of a large language model), releasing of a model checkpoint, or other means that are appropriate to the research performed.
- While NeurIPS does not require releasing code, the conference does require all submissions to provide some reasonable avenue for reproducibility, which may depend on the nature of the contribution. For example
 - (a) If the contribution is primarily a new algorithm, the paper should make it clear how to reproduce that algorithm.
 - (b) If the contribution is primarily a new model architecture, the paper should describe the architecture clearly and fully.
 - (c) If the contribution is a new model (e.g., a large language model), then there should either be a way to access this model for reproducing the results or a way to reproduce the model (e.g., with an open-source dataset or instructions for how to construct the dataset).
 - (d) We recognize that reproducibility may be tricky in some cases, in which case authors are welcome to describe the particular way they provide for reproducibility. In the case of closed-source models, it may be that access to the model is limited in some way (e.g., to registered users), but it should be possible for other researchers to have some path to reproducing or verifying the results.

5. Open access to data and code

Question: Does the paper provide open access to the data and code, with sufficient instructions to faithfully reproduce the main experimental results, as described in supplemental material?

Answer: [\[Yes\]](#)

Justification: We have provided the URL of our code in abstract.

Guidelines:

- The answer NA means that paper does not include experiments requiring code.
- Please see the NeurIPS code and data submission guidelines (<https://nips.cc/public/guides/CodeSubmissionPolicy>) for more details.
- While we encourage the release of code and data, we understand that this might not be possible, so “No” is an acceptable answer. Papers cannot be rejected simply for not including code, unless this is central to the contribution (e.g., for a new open-source benchmark).
- The instructions should contain the exact command and environment needed to run to reproduce the results. See the NeurIPS code and data submission guidelines (<https://nips.cc/public/guides/CodeSubmissionPolicy>) for more details.
- The authors should provide instructions on data access and preparation, including how to access the raw data, preprocessed data, intermediate data, and generated data, etc.
- The authors should provide scripts to reproduce all experimental results for the new proposed method and baselines. If only a subset of experiments are reproducible, they should state which ones are omitted from the script and why.
- At submission time, to preserve anonymity, the authors should release anonymized versions (if applicable).
- Providing as much information as possible in supplemental material (appended to the paper) is recommended, but including URLs to data and code is permitted.

6. Experimental setting/details

Question: Does the paper specify all the training and test details (e.g., data splits, hyper-parameters, how they were chosen, type of optimizer, etc.) necessary to understand the results?

Answer: [\[Yes\]](#)

Justification: All experimental settings, benchmark and training details can be found in Section 5, and Appendix.

Guidelines:

- The answer NA means that the paper does not include experiments.
- The experimental setting should be presented in the core of the paper to a level of detail that is necessary to appreciate the results and make sense of them.
- The full details can be provided either with the code, in appendix, or as supplemental material.

7. Experiment statistical significance

Question: Does the paper report error bars suitably and correctly defined or other appropriate information about the statistical significance of the experiments?

Answer: [\[Yes\]](#)

Justification: All our experimental results come from the average of 1000 training iterations.

Guidelines:

- The answer NA means that the paper does not include experiments.
- The authors should answer “Yes” if the results are accompanied by error bars, confidence intervals, or statistical significance tests, at least for the experiments that support the main claims of the paper.
- The factors of variability that the error bars are capturing should be clearly stated (for example, train/test split, initialization, random drawing of some parameter, or overall run with given experimental conditions).

- The method for calculating the error bars should be explained (closed form formula, call to a library function, bootstrap, etc.)
- The assumptions made should be given (e.g., Normally distributed errors).
- It should be clear whether the error bar is the standard deviation or the standard error of the mean.
- It is OK to report 1-sigma error bars, but one should state it. The authors should preferably report a 2-sigma error bar than state that they have a 96% CI, if the hypothesis of Normality of errors is not verified.
- For asymmetric distributions, the authors should be careful not to show in tables or figures symmetric error bars that would yield results that are out of range (e.g. negative error rates).
- If error bars are reported in tables or plots, The authors should explain in the text how they were calculated and reference the corresponding figures or tables in the text.

8. Experiments compute resources

Question: For each experiment, does the paper provide sufficient information on the computer resources (type of compute workers, memory, time of execution) needed to reproduce the experiments?

Answer: [\[Yes\]](#)

Justification: Experiments compute resources are reported in Section 5.1.

Guidelines:

- The answer NA means that the paper does not include experiments.
- The paper should indicate the type of compute workers CPU or GPU, internal cluster, or cloud provider, including relevant memory and storage.
- The paper should provide the amount of compute required for each of the individual experimental runs as well as estimate the total compute.
- The paper should disclose whether the full research project required more compute than the experiments reported in the paper (e.g., preliminary or failed experiments that didn't make it into the paper).

9. Code of ethics

Question: Does the research conducted in the paper conform, in every respect, with the NeurIPS Code of Ethics <https://neurips.cc/public/EthicsGuidelines>?

Answer: [\[Yes\]](#)

Justification: We fully comply with the NeurIPS Code of Ethics.

Guidelines:

- The answer NA means that the authors have not reviewed the NeurIPS Code of Ethics.
- If the authors answer No, they should explain the special circumstances that require a deviation from the Code of Ethics.
- The authors should make sure to preserve anonymity (e.g., if there is a special consideration due to laws or regulations in their jurisdiction).

10. Broader impacts

Question: Does the paper discuss both potential positive societal impacts and negative societal impacts of the work performed?

Answer: [\[NA\]](#)

Justification: The proposed FlowMoE is a training framework for LLM, thus, has no negative societal impact.

Guidelines:

- The answer NA means that there is no societal impact of the work performed.
- If the authors answer NA or No, they should explain why their work has no societal impact or why the paper does not address societal impact.

- Examples of negative societal impacts include potential malicious or unintended uses (e.g., disinformation, generating fake profiles, surveillance), fairness considerations (e.g., deployment of technologies that could make decisions that unfairly impact specific groups), privacy considerations, and security considerations.
- The conference expects that many papers will be foundational research and not tied to particular applications, let alone deployments. However, if there is a direct path to any negative applications, the authors should point it out. For example, it is legitimate to point out that an improvement in the quality of generative models could be used to generate deepfakes for disinformation. On the other hand, it is not needed to point out that a generic algorithm for optimizing neural networks could enable people to train models that generate Deepfakes faster.
- The authors should consider possible harms that could arise when the technology is being used as intended and functioning correctly, harms that could arise when the technology is being used as intended but gives incorrect results, and harms following from (intentional or unintentional) misuse of the technology.
- If there are negative societal impacts, the authors could also discuss possible mitigation strategies (e.g., gated release of models, providing defenses in addition to attacks, mechanisms for monitoring misuse, mechanisms to monitor how a system learns from feedback over time, improving the efficiency and accessibility of ML).

11. Safeguards

Question: Does the paper describe safeguards that have been put in place for responsible release of data or models that have a high risk for misuse (e.g., pretrained language models, image generators, or scraped datasets)?

Answer: [NA]

Justification: This paper poses no such risks.

Guidelines:

- The answer NA means that the paper poses no such risks.
- Released models that have a high risk for misuse or dual-use should be released with necessary safeguards to allow for controlled use of the model, for example by requiring that users adhere to usage guidelines or restrictions to access the model or implementing safety filters.
- Datasets that have been scraped from the Internet could pose safety risks. The authors should describe how they avoided releasing unsafe images.
- We recognize that providing effective safeguards is challenging, and many papers do not require this, but we encourage authors to take this into account and make a best faith effort.

12. Licenses for existing assets

Question: Are the creators or original owners of assets (e.g., code, data, models), used in the paper, properly credited and are the license and terms of use explicitly mentioned and properly respected?

Answer: [Yes]

Justification: We adhere to the usage restrictions of all assets and correctly cite their sources.

Guidelines:

- The answer NA means that the paper does not use existing assets.
- The authors should cite the original paper that produced the code package or dataset.
- The authors should state which version of the asset is used and, if possible, include a URL.
- The name of the license (e.g., CC-BY 4.0) should be included for each asset.
- For scraped data from a particular source (e.g., website), the copyright and terms of service of that source should be provided.
- If assets are released, the license, copyright information, and terms of use in the package should be provided. For popular datasets, paperswithcode.com/datasets has curated licenses for some datasets. Their licensing guide can help determine the license of a dataset.

- For existing datasets that are re-packaged, both the original license and the license of the derived asset (if it has changed) should be provided.
- If this information is not available online, the authors are encouraged to reach out to the asset's creators.

13. New assets

Question: Are new assets introduced in the paper well documented and is the documentation provided alongside the assets?

Answer: [NA]

Justification: We do not release new assets now, and the code will be open-sourced after the paper is accepted.

Guidelines:

- The answer NA means that the paper does not release new assets.
- Researchers should communicate the details of the dataset/code/model as part of their submissions via structured templates. This includes details about training, license, limitations, etc.
- The paper should discuss whether and how consent was obtained from people whose asset is used.
- At submission time, remember to anonymize your assets (if applicable). You can either create an anonymized URL or include an anonymized zip file.

14. Crowdsourcing and research with human subjects

Question: For crowdsourcing experiments and research with human subjects, does the paper include the full text of instructions given to participants and screenshots, if applicable, as well as details about compensation (if any)?

Answer: [NA]

Justification: We do not involve any crowdsourcing or research with human subjects.

Guidelines:

- The answer NA means that the paper does not involve crowdsourcing nor research with human subjects.
- Including this information in the supplemental material is fine, but if the main contribution of the paper involves human subjects, then as much detail as possible should be included in the main paper.
- According to the NeurIPS Code of Ethics, workers involved in data collection, curation, or other labor should be paid at least the minimum wage in the country of the data collector.

15. Institutional review board (IRB) approvals or equivalent for research with human subjects

Question: Does the paper describe potential risks incurred by study participants, whether such risks were disclosed to the subjects, and whether Institutional Review Board (IRB) approvals (or an equivalent approval/review based on the requirements of your country or institution) were obtained?

Answer: [NA]

Justification: We do not involve any crowdsourcing or research with human subjects.

Guidelines:

- The answer NA means that the paper does not involve crowdsourcing nor research with human subjects.
- Depending on the country in which research is conducted, IRB approval (or equivalent) may be required for any human subjects research. If you obtained IRB approval, you should clearly state this in the paper.
- We recognize that the procedures for this may vary significantly between institutions and locations, and we expect authors to adhere to the NeurIPS Code of Ethics and the guidelines for their institution.

- For initial submissions, do not include any information that would break anonymity (if applicable), such as the institution conducting the review.

16. Declaration of LLM usage

Question: Does the paper describe the usage of LLMs if it is an important, original, or non-standard component of the core methods in this research? Note that if the LLM is used only for writing, editing, or formatting purposes and does not impact the core methodology, scientific rigorousness, or originality of the research, declaration is not required.

Answer: [NA]

Justification: LLMs are not used in any part of the core methodology or scientific content of this work.

Guidelines:

- The answer NA means that the core method development in this research does not involve LLMs as any important, original, or non-standard components.
- Please refer to our LLM policy (<https://neurips.cc/Conferences/2025/LLM>) for what should or should not be described.

Appendix

FlowMoE: A Scalable Pipeline Scheduling Framework for Distributed Mixture-of-Experts Training

Table A.1: Frequently used notations

Name	Description
P	Number of workers (or GPUs) in the cluster.
L	Number of transformer blocks in a MoE model.
B	Number of samples per GPU (or mini-batch size) in one iteration.
N	Number of tokens per sample.
M	Embedding size of a token.
E	Total number of experts per MoE layer.
H	Hidden size of the feed-forward layer in experts.
k	Top- k experts should be selected for each token.
f	Capability factor that determines the maximum number of tokens assigned to each expert.
R	Pipelining degree.
S_p	Partition size of the all-reduce tensor block.
$AT_r^{(l)}$	The r th MHA layer computing subtask of the l th transformer block (including the r th gating subtask)
$E_r^{(l)}$	The r th expert computing subtask of the l th transformer block.
$D_r^{(l)}$	The r th dispatch subtask (A2A communication) of the l th transformer block.
$C_r^{(l)}$	The r th combining subtask (A2A communication) of the l th transformer block.
$AR^{(l)}$	The all-reduce communication task of the l th transformer block during the backward propagation.
$\tau_f(\cdot)/\tau_b(\cdot)$	The beginning execution timestamp of a task during the feed-forward computing/backward propagation.
$t_f(\cdot)/t_b(\cdot)$	The elapsed time of a task during the feed-forward computing/backward propagation.

A Main differences between FlowMoE and the key literature

Table A.2: Main differences between FlowMoE and the key literature on pipeline scheduling for distributed MoE training, where BO represents the Bayesian optimization.

Scheduling framework	vanillaEP[19]	FasterMoE[11]	Tutel[12]	ScheMoE[10]	FlowMoE
A2A pipelining	×	✓	✓	✓	✓
Expert computing pipelining	×	✓	✓	✓	✓
MHA + gating pipelining	×	✗	✗	✗	✓
All-reduce pipelining	×	✗	✗	✗	✓
Auto-tuning	×	✗	✗	✗	✓ (BO)
Robustness of dynamic hardware environment	Weak	Weak	Weak	Weak	Strong
Speedup (Homogeneous 16-GPU cluster)	1.0×	1.28×	1.31×	1.45×	1.82×
Speedup (Heterogeneous 16-GPU cluster)	1.0×	1.31×	1.36×	1.44×	1.74×

B Proof of Theorem 1

According to Eqs. 4 and 5, since the task scheduling timeline in each transformer block is the same and the all-reduce communication time of each transformer block is also the same, we only need to

prove that T_b when inserting $AR^{(l+1)}$ between any two A2A communication tasks of transformer block l will be less than or equal to T_b^* .

We discuss the relationship between T_b and T_b^* under the following four tentative scheduling orders ($1 < l < L, 1 \leq r < R$):

Scheduling order 1: $\tau_b(C_{r+1}^{(l)}) \leq \tau_b(AR^{(l+1)}) \leq \tau_b(C_r^{(l)})$.

Scheduling order 2: $\tau_b(C_1^{(l)}) \leq \tau_b(AR^{(l+1)}) \leq \tau_b(D_R^{(l)})$.

Scheduling order 3: $\tau_b(D_{r+1}^{(l)}) \leq \tau_b(AR^{(l+1)}) \leq \tau_b(D_r^{(l)})$.

Scheduling order 4: $\tau_b(D_1^{(l)}) \leq \tau_b(AR^{(l+1)}) \leq \tau_b(C_R^{(l-1)})$.

If Scheduling order 1 holds, according to Eq. 6b, we have

$$\tau_b(E_r^{(l)}) = \max\{\tau_b(C_r^{(l)}) + t_b(C_r^{(l)}) + t_b(AR^{(l+1)}), \tau_b(E_{(r+1)}^{(l)}) + t_b(E_{(r+1)}^{(l)})\}. \quad (\text{A.1})$$

And if $AR^{(l+1)}$ is performed at the end of backward propagation, according to Eq. 6b, we have

$$\tau_b^*(E_r^{(l)}) = \max\{\tau_b^*(C_r^{(l)}) + t_b(C_r^{(l)}), \tau_b^*(E_{(r+1)}^{(l)}) + t_b(E_{(r+1)}^{(l)})\}. \quad (\text{A.2})$$

Since $\tau_b^*(C_r^{(l)}) = \tau_b(C_r^{(l)})$, according to Eqs. A.1 and A.2, we can derive

$$\tau_b(E_r^{(l)}) \leq \tau_b^*(E_r^{(l)}) + t_b(AR^{(l+1)}). \quad (\text{A.3})$$

Meanwhile, according Eqs. 4, 5 and 6a-6e, we have

$$\tau_b(AR^{(1)}) + t_b(AR^{(1)}) - \tau_b(E_r^{(l)}) + t_b(AR^{(l+1)}) = \tau_b^*(AR^{(1)}) + t_b(AR^{(1)}) - \tau_b^*(E_r^{(l)}). \quad (\text{A.4})$$

In other words, between task $AR^{(1)}$ and task $E_r^{(l)}$, the timeline based on centralized scheduling of all-reduce communication tasks has one more $AR^{(l+1)}$ than the timeline based on Scheduling order 1. Then, adding the left and right terms of Eqs. A.3 and A.4, respectively, we have

$$\tau_b(AR^{(1)}) + t_b(AR^{(1)}) \leq \tau_b^*(AR^{(1)}) + t_b(AR^{(1)}). \quad (\text{A.5})$$

Moreover, since $\tau_b(C_R^{(L)}) = \tau_b^*(C_R^{(L)})$, according to Eq. 6, we have $T_b \leq T_b^*$. An easy-to-understand demonstration is presented in Fig. A.1.

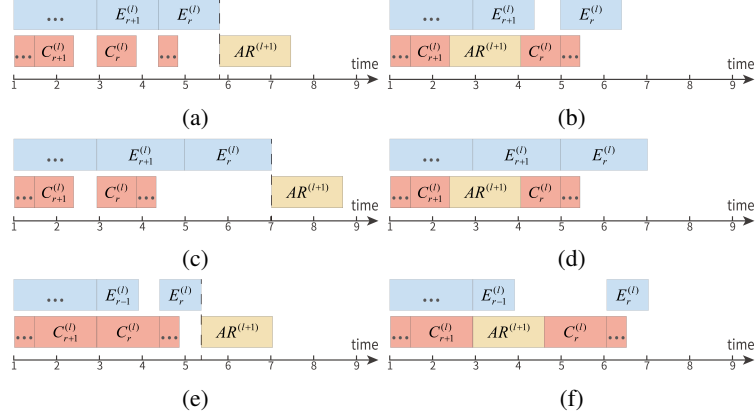


Figure A.1: Demonstration of one example where (a), (c) and (e) represent the three timelines when using centralized scheduling of all-reduce communication tasks (the dotted lines indicate that the tasks before and after do not have direct dependency), and (b), (d) and (f) represent the three timelines when using Scheduling order 1. Comparing (a) with (b), (c) with (d) and (e) with (f), it can be observed that $T_b \leq T_b^*$.

Similarly, we can obtain the same conclusion when using the tentative scheduling orders 2,3 and 4. Therefore, T_b will be less than or equal to T_b^* when inserting all-reduce communication task of one transformer block between any two A2A communication tasks, and the proof is complete.

C Proof of Theorem 2

When the scheduling order satisfies Eqs. 4 and 5 during backward propagation, the idle time of the communication resources (i.e., the gaps between the A2A communication tasks) is fixed if not considering the all-reduce communication tasks. Obviously, the approach to minimize the time of one iteration is to maximize the occupation of the idle time of the communication resources by the communication tasks of the all-reduce tensor chunks. Furthermore, if the communication of the all-reduce tensor chunks does not introduce extra startup overhead, the total time of the all-reduce communication tasks will remain unchanged for different S_p . When S_p is larger, A2A communication tasks may not be executed in time due to uncompleted communication tasks of the all-reduce tensor chunks, which will cause the timeline of the computing tasks to shift back according to Eqs. 6b and 6d and part of the communication tasks of the all-reduce tensor chunks do not occupy the free time of the communication resource (see Figs. A.1b and A.1f). On the contrary, when $S_p \rightarrow 0$, the communication tasks of the all-reduce tensor chunks will not affect the timeline of the A2A communication tasks and thus will not change the timeline of the computing tasks due to the higher priority of the A2A communication tasks. Meanwhile, it will maximize the free time of the communication resources. Thereby, the proof is complete.

D Design and Performance Evaluation of BO

D.1 Parameter Settings and Advantage Analysis

We choose BO to obtain a near-optimal S_p benefiting from the following three points:

- First, BO is not limited by the expression of the objective function (we use $\mathcal{F}(S_p)$ as the objective function) and depends only on the sampling values obtained (i.e., $\hat{\mathcal{F}}(S_p^1), \hat{\mathcal{F}}(S_p^2), \dots, \hat{\mathcal{F}}(S_p^n)$). We use Gaussian process regression with the Matern kernel to predict the value of the objective function as it is commonly used as a good surrogate model for BO [49]. A 95% confidence interval is associated with $\mathcal{F}(S_p)$, which is considered the most likely region for the value of $\mathcal{F}(S_p)$.
- Second, BO typically requires only a limited number of trials to find high-quality solutions, resulting in low search overhead. To minimize the number of trials, it selects the next configuration S_p by maximizing an acquisition function [49]. In FlowMoE, we adopt the Expected Improvement (EI) acquisition function to choose the S_p that can maximize training speedup improvement compared to the current best result.
- Third, BO avoids the search process from falling into a local optimum by tuning the hyperparameter Expected Improvement (EI). Specifically, a smaller EI favors exploitation, i.e., collecting more points near the peak, while a larger EI tends to exploration, i.e., collecting more scattered points in the range [49]. In FlowMoE, we choose EI=0.1 to prefer S_p exploration, which is a commonly adopted value [31, 50]. Meanwhile, the search space of S_p in BO can be set as [0MB, the maximum value of the tensor to be communicated in each transformer block] and the required one initial sample value is randomly generated, which can effectively cover the optimal S_p for different hardware clusters and MoE models, e.g., from 0MB-10MB in Fig. 4.

D.2 Importance Analysis of BO

BO auto-tuning is an indispensable part of FlowMoE and is absolutely necessary. The performance of FlowMoE depends on the introduced BO process. Specifically, an oversized all-reduce tensor chunk will affect the prioritization of A2A communication tasks and may prevent them from being started in time. In contrast, an undersized all-reduce tensor chunk will result in excessive startup overhead. Therefore, neither an oversized nor undersized all-reduce tensor chunk can achieve the shortest per-iteration time, and there must exist a unique optimal solution that maximizes training speed. The BO optimizer balances these two competing effects by sampling and learning from actual iterations, efficiently finding an all-reduce tensor chunk size that maximizes overlap without incurring excessive overhead. This tuning is crucial because the optimal trade-off point varies across models, GPU interconnect topologies, and MoE configurations.

D.3 Performance Evaluation of BO

Table A.3: Comparison of average per-iteration time in milliseconds when using different approaches to tune the partitioning size S_p .

Model	Time (ms)			
	BO	Grid Search	Random Number Generation	
GPT2-Tiny-MoE	95.6	101.3	109.3	
BERT-Large-MoE	351.9	373.80	388.96	
LLaMA2-MoE	1124.0	1208.23	1250.09	
DeepSeek-v2-S	3205.3	3498.8	3902.75	

We compare the performance of BO with the other two methods including grid search and random number generation on tuning S_p . In our experiments, we set the other two methods to use the same search space as BO. For grid search, the search space is divided into 8 equal parts to construct 8 discrete sampling points. Similarly, the grid search utilized the first 80 iterations of the training process to determine S_p . Specifically, each iteration time corresponding to each sample point is obtained by averaging 10 iterations, and the sample point corresponding to the smallest per-iteration time is used as the value of S_p for subsequent training. For random number generation, we randomly selected a number from the search space as the value of S_p in each iteration. Table A.3 shows the comparison of average iteration times when using different methods of tuning S_p in FlowMoE on Cluster 1 with 16 GPUs. It can be observed that using BO to tune S_p obtained the shortest per-iteration time among the three methods. Although grid search obtains better performance than random number generation, its limited number of sampling points makes it difficult to cover the optimal solution especially when the search space is large, and over-increasing the number of sampling points brings higher search overhead and longer search process. On the contrary, BO can obtain a near-optimal S_p with very little overhead, and therefore we choose it.

Table A.4: Comparison of average per-iteration time in milliseconds when using FlowMoE with BO auto-tuning or different fixed partition sizes.

Model	Time (ms)					
	BO	$S_p=0.5\text{MB}$	$S_p=1\text{MB}$	$S_p=2\text{MB}$	$S_p=4\text{MB}$	$S_p=8\text{MB}$
GPT2-Tiny-MoE	95.6	130.1	115.9	104.7	109.7	122.3
BERT-Large-MoE	351.9	388.9	378.6	362.2	386.3	395.1
LLaMA2-MoE	1124.0	1213.8	1167.9	1185.9	1211.8	1240.5
DeepSeek-v2-S	3205.3	4438.5	3948.9	3654.7	3493.9	3740.2

BO Auto-tuning v.s. Different Fixed Partition Sizes. In addition, we count the average per-iteration time when using FlowMoE with BO auto-tuning or different fixed partition sizes for training four MoE models (see Table 2 for their detailed configurations) in Cluster 1 with 16 GPUs to validate the sensitivity of FlowMoE to S_p . As shown in Table A.4, different partition sizes greatly affect the training efficiency and BO auto-tuning is essential to maximize the performance of FlowMoE.

Table A.5: Comparison of average per-iteration time when training BERT-Large-MoE with different BO parameter configurations on Cluster 1, where the surrogate model uses Gaussian Process Regression (GPR) with different kernel functions.

BO Hyperparameter	Surrogate Model	Time (ms)
Acquisition Function		
Expected Improvement (EI=0.1)	GPR + Matern	351.9
Expected Improvement (EI=0.05)	GPR + Matern	358.9
Expected Improvement (EI=0.2)	GPR + Matern	354.2
Probability of Improvement	GPR + Matern	355.1
Lower Confidence Bound	GPR + Matern	355.4
Expected Improvement (EI=0.1)	GPR + RBF	357.2
Expected Improvement (EI=0.1)	GPR + Rational Quadratic	360.2

Sensitivity of BO hyperparameters. In FlowMoE, the objective function for per-iteration time regarding the all-reduce tensor chunk size is a single-peaked, smooth objective function with a fixed search space. For this objective function, the process of using BO to find the optimal solution is insensitive to the two hyperparameters (acquisition function and surrogate model) of BO, and BO always converges and approaches the optimal solution. Table A.5 shows the comparison results of average per-iteration time when training BERT-Large-MoE with different BO parameter configurations on Cluster 1. The results indicate that although the performance of FlowMoE is sensitive to the BO process, BO hyperparameters have a minor impact on it, and different BO configurations lead to similar iteration time.

Table A.6: Percentage of the computational overhead of BO to the training time of first 1000 iterations.

Model	GPT2-Tiny-MoE	BERT-Large-MoE	LLaMA2-MoE	DeepSeek-v2-S
Overhead	3.22%	1.38%	0.43%	0.16%

Computational Overhead of BO. We also measure the percentage of the computational overhead of BO to the training time of first 1000 iterations when training four MoE models. The experimental results are illustrated in Table A.6. It can be observed that this overhead is negligible compared to the gains brought by BO (see Table 3), and it will be smaller when training the model to convergence, which involves tens of thousands of iterations. Thus, the auto-tuning process of BO is lightweight and practical.

E Algorithm Description and Scalability Analysis

Algorithm 1 describes the pipeline of R -degree computing and communication tasks during the training process. Line 1-4 initializes the necessary parameters and queues. Line 6-12 performs the feed-forward computing of each iteration according to Eqs. 2 and 3. Meanwhile Line 13-21 performs the backward propagation of each iteration according to Eqs. 4 and 5. Algorithm 2 shows the management in the communication pool. The PARTITION procedure is responsible for splitting the tensor of the MHA layer and gating function during the backward propagation process and placing it into the queue of the all-reduce communication tasks. The COMMPOOLMANAGER procedure performs the two types of communication tasks according to the defined priorities, where Line 9-11 prioritizes the execution of the A2A communication tasks and queues the data obtained after the communication, while Line 12-13 executes the communication tasks of the all-reduce tensor chunks when there are no A2A communication tasks.

To analyze the scalability of FlowMoE’s scheduling algorithm, we examine the computational complexity of each iteration of the MoE model in distributed training. We assume that each GPU processes the same number of tokens and do not consider the non-overlapped time of A2A communication and all-reduce communication in each iteration, then the time complexity of one iteration is $\mathcal{O}(L \times [BNM^2 + B^2N^2M + BNME + 2BNMH])$, where $\mathcal{O}(BNM^2 + B^2N^2M)$ denotes the linear mapping of the Q,K,V and linear transformation matrix in the MHA layer and the attention score computation, $\mathcal{O}(BNME)$ denotes the gate function computing with the structure of $M \times E$, and $\mathcal{O}(2BNMH)$ denotes the expert computing on each GPU. Then, when the complexity of the MoE model scales up, the increase in the complexity of FlowMoE’s scheduling algorithm is significantly smaller than the increase in the complexity of one iteration time. Meanwhile, when the number of GPUs P in the cluster increases, the complexity of the scheduling algorithm of FlowMoE is not affected, but the complexity of one iteration time may increase due to the longer time of the communication tasks. In summary, the ratio of the time overhead of FlowMoE’s scheduling algorithm to one iteration time will decrease when the model complexity and the number of GPUs increase. Therefore, FlowMoE’s scheduling algorithm has good scalability.

F System Description

From the closest to user level to the lowest level, distributed training frameworks and communication stacks usually include: User Script level, PyTorch frontend with high-level APIs, PyTorch Engine, message-level communication library. To ensure the generality of FlowMoE, we can not modify user scripts and framework engines heavily. However, due to the diversity of MPI (e.g., OpenMPI [51],

Intel MPI [52]) and network interfaces (e.g., Ethernet, Infiniband) in the communication library level, it is almost impossible to make one piece of code work in all communication libraries. Therefore, FlowMoE is deployed at the PyTorch API level, where its four modules is elaborated as follow:

- Task Breakdown Manager is responsible for splitting the dataset of each batch size according to the degree R and requesting different communication/computing subtasks based on the tensor transferred between different computing and communication tasks. Task Breakdown Manager has been improved based on Tutel.
- BO autotuner is responsible for searching the near-optimal partition size and guiding the partitioning of the all-reduce tensor.
- Communication Task Pool maintains queues of A2A communication tasks and all-reduce chunk communication tasks. On the one hand, it receives A2A communication tasks requested from the Task Breakdown Manager and queues them according to the request order. On the other hand, it splits the all-reduce tensor generated in the backward propagation and queues the all-reduce chunks.
- Pipeline Scheduling Manager submits the requested multiple computing tasks and communication tasks in the queue to the PyTorch Engine and the communication library according to the defined scheduling order and priority.

In addition, the backward propagation of each transformer block is not intuitively visible in PyTorch, and the gradients of the model parameters can only be accessed after the backward propagation is fully completed. To obtain the gradient tensors of the MHA layer and gating function for each transformer block in time during backward propagation, we use `register_full_backward_hook` to access the gradients and split the gradient tensors into queues based on the partition size S_p . Meanwhile, we achieve the overlapping of computing and communication tasks by using multi-threading. Specifically, the main thread includes Task Breakdown Manager, BO autotuner and Pipeline Scheduling Manager and is responsible for scheduling all tasks. We also create one sub-thread in Communication Task Pool to schedule the communication tasks in the two queues based on the defined priorities, and a `threading.Lock` is used to maintain security for all threads.

G Stress Tests in two Scaled-up MoE Models

Table A.7: Comparison of average per-iteration time when training two scaled-up MoE models. S1, S2, and S3 are the speedups of FlowMoE over ScheMoE, Tutel and vanillaEP, respectively.

# of GPUs	Model	Time (ms)				S_3	S_2	S_1
		vanillaEP	Tutel	ScheMoE	FlowMoE			
4	LLaMA2-MoE-L	2405.1	1927.0	1806.1	1493.8	$1.61 \times 1.29 \times 1.21 \times$		
	DeepSeek-V2-M	535.3	468.4	432.2	352.2	$1.52 \times 1.33 \times 1.23 \times$		
8	LLaMA2-MoE-L	2989.1	2493.9	2297.9	1833.8	$1.63 \times 1.36 \times 1.25 \times$		
	DeepSeek-V2-M	944.6	773.4	723.6	552.4	$1.71 \times 1.40 \times 1.31 \times$		
16	LLaMA2-MoE-L	OOM	OOM	OOM	OOM	/	/	/
	DeepSeek-V2-M	1254.6	956.9	893.4	708.8	$1.77 \times 1.35 \times 1.26 \times$		

To stress-test FlowMoE’s performance, we measured the training performance of different training frameworks on two scaled-up MoE models (LLaMA2-MoE-L and DeepSeek-V2-M), both of which are close to the memory upper limit of Cluster 1. Table A.7 shows the average per-iteration time using different frameworks on these two MoE models (FasterMoE is OOM in any cases). The results indicate that FlowMoE still achieved the best training performance among all baselines on larger models.

H Convergence Analysis and Experiments

We denote the samples processed in each pipeline as one microbatch, and the number of microbatches is equal to the pipelining degree R .

Specifically, during the backpropagation of the l th transformer block in one iteration, the gradients from all AT_r^l and E_r^l ($1 \leq r \leq R$) after backpropagation are accumulated and summed. Once the gradient from AT_1^l is also accumulated, the All-Reduce chunk communication task for the MHA and gate function in the l th transformer block is started. Similarly, when the gradient of E_1^l is accumulated, the expert parameters are updated. This effectively prevents the parameters of MHA, the gate function, and the expert from being updated early, thereby avoiding gradient staleness. Additionally, to ensure that the accumulated gradients are equivalent with and without pipelining, we scale the loss calculated for each microbatch by R , i.e., $\frac{loss^{(r)}}{R}$ ($1 \leq r \leq R$), where $loss^{(r)}$ is the loss calculated using the samples from the r th microbatch, and the detailed theoretical derivation is as follows:

The loss and gradient when performing backpropagation using the entire mini-batch are expressed as follows:

$$loss = \frac{1}{B} \sum_{i=1}^B \ell(x_i, y_i), \nabla L_{full} = \nabla \left(\frac{1}{B} \sum_{i=1}^B \ell(x_i, y_i) \right), \quad (\text{A.6})$$

which is currently used by all mainstream MoE training frameworks [12, 38, 28].

When dividing mini-batch into R microbatches, the number of samples in each microbatch is $b = \frac{B}{R}$. The loss for each microbatch is:

$$loss^{(r)} = \frac{1}{b} \sum_{i=1}^b \ell(x_{r,i}, y_{r,i}). \quad (\text{A.7})$$

Then, the scaled loss for each microbatch is:

$$\tilde{loss}^{(r)} = \frac{1}{R} \cdot loss^{(r)} = \frac{1}{R} \cdot \frac{1}{b} \sum_{i=1}^b \ell(x_{r,i}, y_{r,i}) = \frac{1}{B} \sum_{i=1}^b \ell(x_{r,i}, y_{r,i}). \quad (\text{A.8})$$

The cumulative loss of all microbatches is:

$$\sum_{r=1}^R \tilde{loss}^{(r)} = \sum_{r=1}^R \frac{1}{B} \sum_{i=1}^b \ell(x_{r,i}, y_{r,i}) = \frac{1}{B} \sum_{r=1}^R \sum_{i=1}^b \ell(x_{r,i}, y_{r,i}) = \frac{1}{B} \sum_{i=1}^B \ell(x_i, y_i). \quad (\text{A.9})$$

According to Eqs. A.11 and A.8, we can obtain:

$$\nabla \left(\sum_{r=1}^R \tilde{loss}^{(r)} \right) = \nabla \left(\frac{1}{B} \sum_{i=1}^B \ell(x_i, y_i) \right) = \nabla L_{full}. \quad (\text{A.10})$$

This analysis shows that the gradient update strategy is numerically equivalent with and without pipelining. The only difference between them is the optimization of task scheduling order during execution, which does not compromise model convergence during training.

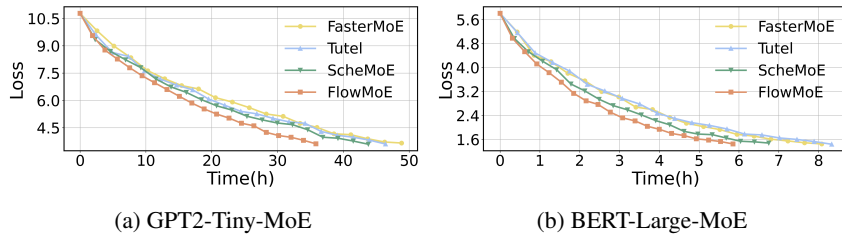


Figure A.2: Loss with time for training GPT2-Tiny-MoE and BERT-Large-MoE.

Furthermore, we experimentally verify the convergence of FlowMoE by training GPT2-Tiny-MoE and BERT-Large-MoE on Cluster 1 with 16 GPUs. As shown in Fig. A.2, FlowMoE reaches the same loss as the baselines, and it takes much less time due to reduced per-iteration time.

I Performance Lower Bound Analysis

We analyze the performance lower bound of FlowMoE from the following three cases:

- (1) **The communication task time is much longer than the computing task time.** When the communication time is very long, the time of the All-to-All (A2A) communication task alone completely covers the computing task time. In this case, the All-Reduce (AR) chunk based priority scheduling mechanism will fail because the AR chunk cannot be inserted into the A2A communication task. The performance of FlowMoE will be the same as ScheMoE, Tutel, and FasterMoE, but better than vanillaEP due to the hidden computing task time.
- (2) **The computing task time is much longer than the communication task time.** When the computing time is very long, all the communication task time can be covered by the computing task time. In this case, FlowMoE will outperform ScheMoE, Tutel, and FasterMoE due to the hidden AR task time, and better than vanillaEP because it further hides the A2A task time.
- (3) **The communication task time is comparable to the computing task time.** In this case, FlowMoE outperforms all baselines because it maximizes the overlap of multi-type tasks.

In summary, in all cases, the performance of FlowMoE is greater than or equal to that of ScheMoE, Tutel, and FasterMoE, and is always better than that of vanillaEP.

J GPU SM Utilization

Table A.8: Average GPU SM utilization with different microbatch sizes.

Name	Model	R	Average GPU SM Utilization
FlowMoE	GPT2-Tiny-MoE	2	72.63%
FlowMoE	GPT2-Tiny-MoE	4	48.43%
vanillaEP	GPT2-Tiny-MoE	/	87.09%
FlowMoE	BERT-Large-MoE	2	87.84%
FlowMoE	BERT-Large-MoE	4	78.16%
vanillaEP	BERT-Large-MoE	/	88.90%
FlowMoE	LLaMA2-MoE	2	89.16%
FlowMoE	LLaMA2-MoE	4	88.19%
vanillaEP	LLaMA2-MoE	/	89.49%
FlowMoE	DeepSeek-V2-S	2	89.27%
FlowMoE	DeepSeek-V2-S	4	88.85%
vanillaEP	DeepSeek-V2-S	/	90.77%

First, we use the CUPTI tool to measure GPU SM utilization on Cluster 1 with 16 GPUs under different microbatch sizes. Specifically, we adjust the microbatch size by changing the pipelining degree R (a larger R results in a smaller microbatch). VanillaEP represents the original mini-batch without pipelining. The results are shown in Table A.8. We observe that smaller microbatch sizes may result in lower GPU SM utilization (e.g., when training GPT2-Tiny-MoE with $R = 4$ using FlowMoE), but in most cases, GPU SM utilization is nearly identical to that without pipelining (e.g., when training BERT-Large-MoE, LLaMA2-MoE and DeepSeek-V2-S using FlowMoE). This is because the actual tensors involved in GPU computation remain sufficiently large for larger MoE models, and GPU SM resources are still utilized efficiently. In other words, the microbatches introduced by FlowMoE’s pipelining do not waste GPU SM resources for large MoE models.

Second, we measure GPU SM utilization with different batch sizes when training different MoE models using FlowMoE on Cluster 1 with 16 GPUs. As illustrated in Table A.9, smaller batch sizes are more likely to lead to lower GPU SM utilization, e.g., when training GPT2-Tiny-MoE or BERT-Large-MoE with a batch size of 2. Moreover, GPU SM utilization remained nearly unchanged when training LLaMA2-MoE or DeepSeek-V2-S. This is because these two MoE models have a larger number of parameters, which keeps the tensor dimensions involved in GPU computation sufficiently large, ensuring that SM resources are still efficiently utilized even with a lower batch size.

Table A.9: Average GPU SM utilization with different batch sizes when using FlowMoE.

Model	Batch Size	Average GPU SM Utilization
GPT2-Tiny-MoE	4	72.63%
GPT2-Tiny-MoE	2	36.62%
BERT-Large-MoE	4	87.84%
BERT-Large-MoE	2	61.48%
LLaMA2-MoE	4	89.16%
LLaMA2-MoE	2	88.45%
DeepSeek-V2-S	4	89.27%
DeepSeek-V2-S	2	89.06%

Table A.10: Parameter Configurations for BERT-Large-MoE-w

MoE Model	# Params (MHA+Gating)	# Params (Experts)	Dataset	Configurations				
				L	B	N	M	H
BERT-Large-MoE-w	25.2M	3325.9M	wikitext-103	24	4	512	512	1024
				8				1

Table A.11: The maximum and minimum GPU SM utilization for a large number of experts with different numbers of activated experts when using FlowMoE in Cluster 1 with 16 GPUs..

Model	f	Maximum GPU SM Utilization	Minimum GPU SM Utilization
BERT-Large-MoE-w	1.0	89.20%	87.81%
BERT-Large-MoE-w	4.0	89.72%	50.65%
BERT-Large-MoE-w	8.0	90.30%	31.60%
BERT-Large-MoE-w	16.0	90.68%	19.41%

Third, we also evaluate the impact of the number of activated experts on GPU utilization when using FlowMoE on Cluster 1 with 16 GPUs for a large number of experts. Specifically, we construct BERT-Large-MoE-w by increasing the number of experts per GPU from 2 to 8 and adjusting the number of activated experts by modifying the capacity factor f , where a larger f indicates more uneven token routing by the gate function and fewer activated experts since most tokens are routed to popular experts. The detailed configurations of BERT-Large-MoE-w are shown in Table A.10. We use the CUPTI tool and report the maximum and minimum GPU SM utilization in Table A.11. The results demonstrate that, with a large number of experts, the fewer the number of activated experts, the more unbalanced the computation load on the GPU and the greater the difference in SM utilization between GPUs.

K Robustness Analysis

We discuss the robustness of FlowMoE to heterogeneous clusters, dynamic hardware environments, and node dropouts.

K.1 Robustness for Heterogeneous Clusters

Table A.12: Comparison of average iteration time in milliseconds when the GPUs have different computing power. S_1 , S_2 , S_3 and S_4 are the speedups of FlowMoE over vanillaEP, FasterMoE, Tutel and ScheMoE, respectively.

Model	Time (ms)					S_4	S_3	S_2	S_1
	vanillaEP	FasterMoE	Tutel	ScheMoE	FlowMoE				
GPT2-Tiny-MoE	235.8	201.6	189.1	178.2	153.3	$1.54 \times 1.32 \times 1.23 \times 1.16 \times$			
BERT-Large-MoE	657.7	608.7	590.8	500.6	449.2	$1.46 \times 1.36 \times 1.31 \times 1.11 \times$			
LLaMA2-MoE	2439.1	2152.2	1849.2	1707.4	1468.3	$1.66 \times 1.47 \times 1.26 \times 1.15 \times$			
DeepSeek-V2-S	7233.7	5495.1	5323.0	4958.3	4142.4	$1.74 \times 1.33 \times 1.28 \times 1.20 \times$			

We conduct a detailed analysis on how FlowMoE adapts to heterogeneous GPU clusters. (1) **For clusters with mixed GPU types**, since all-reduce and A2A tasks can only begin once the slowest GPU completes its corresponding computing task (other GPUs will be idle in waiting time after completing their computing tasks), the task timeline for each iteration of FlowMoE and other baselines is determined by the slowest GPU. In this case, FlowMoE can maximize the computing/communication overlap of the slowest GPU, and its performance still outperforms the baselines. To verify this conclusion, we construct a heterogeneous cluster with 16 GPUs on Cluster 1 with different GPU types. We add delay to each iteration on 8 GPUs in one node of Cluster 1 to simulate the computing power reduction. Specifically, we use `register_forward_hook` and `register_hook` in PyTorch to access the forward computing and backward propagation of each layer. Meanwhile, we synchronize the tensor of each layer with `torch.cuda.synchronize` after it completes the forward computing or gradient computing. Then, we obtain the forward computing or backward propagation time of each layer according to the interval between two tensor synchronizations and inject equivalent delays during both passes, which effectively simulates halving the computing power of the GPUs. Table A.12 demonstrates that FlowMoE still obtains the shortest end-to-end training time when the GPUs have different computing power. (2) **For clusters with bandwidth asymmetry**, since AR and A2A tasks are collective communications, all GPUs start and finish communication tasks simultaneously regardless of whether their bandwidths are the same. Therefore, the task scheduling timeline is the same for all GPUs. In this case, FlowMoE still achieves better performance than the baseline due to its efficient pipeline solution.

K.2 Robustness for Dynamic Hardware Environments

In real large-scale training clusters, the hardware environments including network bandwidth and GPU computing power may change dynamically. To address it, we design the re-Bayesian tuning mechanism for FlowMoE and BO will be automatically re-executed when the hardware environment changes. Specifically, we define a re-execution threshold δ . We denote the iteration time corresponding to the near-optimal S_p predicted by the last BO as $\hat{\mathcal{F}}(S_p^{best})$. If the change of the current iteration time T compared to $\hat{\mathcal{F}}(S_p^{best})$ is more than δ , i.e.,

$$\frac{|T - \hat{\mathcal{F}}(S_p^{best})|}{\hat{\mathcal{F}}(S_p^{best})} > \delta, \quad (\text{A.11})$$

the BO will be re-executed to find a new S_p .

K.3 Robustness for Node Dropouts

In FlowMoE, to improve the fault tolerance of the system to handle node dropouts, we adopt the following approach:

First, a replica of each expert parameter is stored separately on two different nodes to ensure that when a node fails, its corresponding expert parameter can still continue to be served by the backup replica. To ensure the parameter consistency between the replicas, we set to synchronize the updating of expert parameters every fixed number of iteration steps (e.g., every 1000 steps) during the training process.

Second, FlowMoE periodically calls `torch.distributed.barrier()` during the training process with a reasonable timeout (e.g., 5 minutes). When a synchronization operation times out and throws an exception, we determine that a node has failed, and obtain the rank of the failed node from the exception information. Then, FlowMoE will execute the following recovery process:

- (1) Based on the node replica information, the gating function routing table is updated on all surviving nodes, and the requests originally assigned to the faulty node are remapped to its corresponding backup node;
- (2) The remaining surviving nodes are adapted to the new set of nodes and subsequently trained by destroying the current communication group (`dist.destroy_process_group()`) and reinitializing a new distributed communication group (`dist.init_process_group()`);

Therefore, FlowMoE is able to effectively handle the risks from node dropouts in large-scale distributed training, and improves the stability and reliability of the overall training.